Single-particle energies in neutron-rich nuclei by shell model sum rule

A. Umeya and K. Muto
Department of Physics, H-33, Tokyo Institute of Technology, Meguro, Tokyo, 152-8551, Japan
(Received 27 April 2006; published 27 September 2006)

One of the most striking features in neutron-rich nuclei is the disappearance of magic number $N = 8$ or 20, which indicates a change of single-particle energy spectra and the disappearance of a large energy gap at the magic number. A sum-rule method is formulated, based on the shell model, for the evaluation of single-particle energies. It is shown that the triplet-even central component of the NN interaction plays a decisive role through the monopole interaction for a change of single-particle energy spectra, leading to a rapid decrease of the energy gap at $N = 8$ and 20. The triplet-even attraction is due partly to the original central interaction and partly to the second-order tensor correlations of the one-pion exchange potential. A multipole expansion analysis of NN interactions shows that the contribution to the single-particle energy from the monopole interactions between two orbits depends on the nodal quantum numbers of the orbits.

DOI: 10.1103/PhysRevC.74.034330 PACS number(s): 21.60.Cs, 21.30.Fe, 27.20.+n

I. INTRODUCTION

Attempts at understanding the structure of atomic nuclei have been made since the 1930s. Many experiments of nuclei have been carried out so far, and many nuclei have been discovered and investigated. At present, we know the existence of about 270 stable nuclei, about 50 naturally occurring radioactive isotopes, and about 2500 unstable nuclei. These nuclei, however, have not occupied even half of the nuclear chart. There are about 4000 nuclei that have yet to be discovered. Most of these nuclei are neutron-rich nuclei. It is expected that these nuclei would have exotic properties, and studies of these nuclei might give us new concepts on nuclear structures. In addition, these nuclei are important for understanding the mechanism of nucleosynthesis in supernovae, that is, the rapid neutron-capture process (r-process). In the r-process, nuclei heavier than Fe are created through a region of neutron-rich nuclei in the nuclear chart.

In recent years, experiments on neutron-rich nuclei have been carried out owing to the development of experimental techniques. In the light-mass region, most of the nuclei have been investigated. They have shown characteristic properties of neutron-rich nuclei that are different from those of stable nuclei. One of the most striking features of neutron-rich nuclei is the disappearance of the magic numbers that have been established in stable nuclei. For example, the neutron number $N = 8$ is not a magic number at proton number $Z = 3, 4$ [1–5], and $N = 20$ is not at $Z = 9$–12 [6–9]. Additionally, it is suggested that the magic numbers $N = 14$ and $N = 16$ appear near the neutron drip line [8,10]. This indicates a change of single-particle energy spectra and the disappearance of a large energy gap at $N = 8$ and $N = 20$ in those nuclei with a large neutron excess.

Single-particle energies of nucleons in a nucleus are mainly determined by interactions among nucleons. Theoretical calculations of single-particle energies have been carried out for neutron-rich nuclei [11–15]. A qualitative description of the shell evolution with proton number based on experimental evidence toward the neutron-rich region has been given for p, sd, and fp shells in Ref. [16]. Recently, it was suggested by theoretical considerations that the spin-isospin $(\boldsymbol{\sigma}\cdot\boldsymbol{\sigma})(\boldsymbol{\tau}\cdot\boldsymbol{\tau})$ component of the NN interaction between spin-orbit partners, $j = \ell \pm 1/2$, is responsible for the energy gap at the magic numbers [14]. However, there seems to be no theoretical research that verifies the importance of the spin-isospin interaction for the appearance of magic numbers.

The purpose of this study is to clarify the mechanism changing single-particle energy spectra with proton number in the neutron-rich region, by analyzing contributions of different components of NN interactions to the single-particle energies. We define a single-particle energy for open-shell nuclei in terms of spectroscopy, and we derive a monopole interaction from the spectroscopic definition by using a sum-rule method based on the shell model. We demonstrate that the large energy gaps that correspond to the magic numbers become narrower as the proton number decreases in the p-shell region and sd-shell region. In addition, by analyzing the empirical matrix elements of NN interactions, we show that the triplet-even component of the neutron-proton interactions determines the change of neutron single-particle energy spectra with decreasing proton number. In the effective interaction, the triplet-even component has the strongest attractive potential because of the tensor force that arises mainly from one-pion exchange. We demonstrate the mechanism for the deuteron case. As a qualitative discussion, we analyze the central force of NN interaction using a multipole expansion and evaluate the monopole interaction.

In our previous papers [17–19], we showed a result of the shell-model sum-rule method, that is, the single-particle energy that is represented by the monopole interaction, and we did not describe any details of the sum-rule method. Numerical results and brief discussions were given for the single-particle energies in only the p-shell region. In this paper, we explain details of the shell-model sum rule and analyses of NN interactions, and we show the numerical applications in the p- and sd-shell regions.

In Sec. II, we show experimental evidence of the disappearance of magic numbers. In Sec. III, we define a single-particle energy for open-shell nuclei in terms of spectroscopy and

introduce a shell-model sum-rule method. In Sec. IV, we show a derivation of the monopole interaction by applying the sum rule to a shell-model Hamiltonian. The calculated results for nuclei in the p- and sd-shell regions are shown in Sec. V. In Sec. VI, we discuss the monopole interaction from several viewpoints. In Sec. VI A, we show that the monopole interaction often appears in nuclear structure calculations. In Sec. VI B, we point out the important role of the triplet-even component by decomposing NN interactions. The origin of the triplet-even attraction is discussed in Sec. VI C. In Sec. VI D, we compare our results with calculations by Otsuka *et al.* [14] and comment on the spin-isospin $(\boldsymbol{\sigma}\cdot\boldsymbol{\sigma})(\boldsymbol{\tau}\cdot\boldsymbol{\tau})$ component. A qualitative discussion of the monopole interaction obtained by applying a multipole expansion is given in Sec. VI E. In Sec. VI F, the effect of the Coulomb force for proton single-particle energy is discussed. Conclusions are given in Sec. VII.

II. EXPERIMENTAL EVIDENCE

One piece of evidence for the disappearance of magic numbers can be seen in the systematics of neutron separation energies, which are shown in Fig. 1. The neutron separation energy is defined as

$$S_n(N,Z) = B(N,Z) - B(N-1,Z), \tag{1}$$

where $B(N,Z)$ is the binding energy of a nucleus with N neutrons and Z protons. In Fig. 1, the lines connect nuclides with the same neutron excess $N-Z$. A closed-shell nucleus is specially stable. When one nucleon is added to the closed-shell nucleus, the last nucleon on the next shell is loosely bound. The separation energies thus decrease immediately after the magic number. The neutron number $N=8$ is clearly a magic number on the $N-Z=1$ line, but $N=8$ is not a magic number on the $N-Z=3,5$ lines. Similarly, the neutron number $N=20$ is a magic number on the $N-Z=1,3,5$ lines, but $N=20$ is not on the $N-Z=7,9$ lines. In addition, the neutron number $N=16$ becomes a magic number on the $N-Z=5,7$ lines;

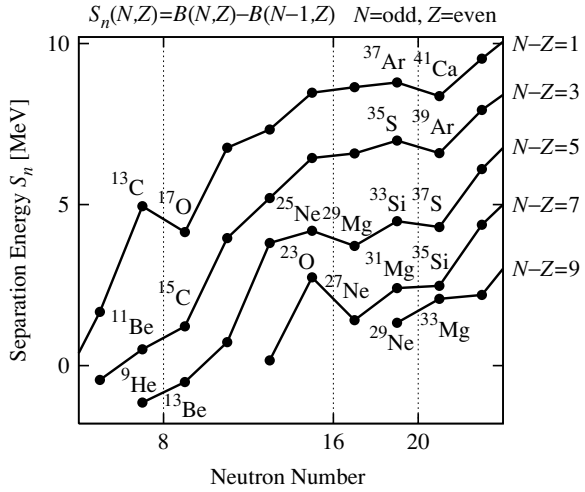

FIG. 1. Neutron separation energies for light nuclei (odd N and even Z) [20].

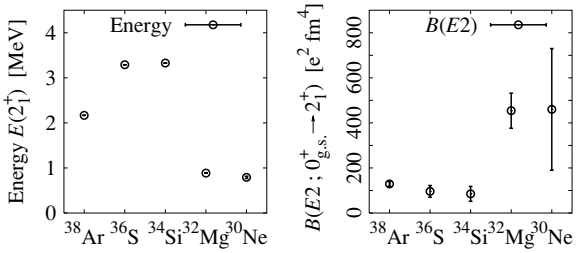

FIG. 2. Measured $E(2_1^+)$ (left) and $B(E2;0^+_{g.s.}\rightarrow 2^+_1)$ (right) values for $N=20$ isotones [7,9,21–23].

that is, the appearance of a new magic number $N=16$ in neutron-rich nuclei is suggested.

For the magic number $N=20$, another piece of evidence can be seen in the first 2^+ energies $E(2_1^+)$ and reduced $E2$ transition probabilities $B(E2;0^+_{g.s.}\rightarrow 2^+_1)$. Raman *et al.* gave a systematic analysis of $E(2_1^+)$ and $B(E2)$ for even-even nuclei [21,24,25]. Their analysis suggests that the first 2^+ excited state of nuclei with a magic number has a large excitation energy. Additionally, the reduced $E2$ transition probability from ground 0^+ state to 2^+ state is small. In Fig. 2, the measured $E(2_1^+)$ values for ^{30}Ne and ^{32}Mg are smaller than for the other $N=20$ isotones. Measured $B(E2)$ values for ^{30}Ne and ^{32}Mg are larger than those for the other $N=20$ isotones. The $N=20$ nuclei ^{34}Si, ^{36}S, and ^{38}Ar have spherical shape. In contrast, neutron-rich nuclei ^{30}Ne and ^{32}Mg have large deformation in spite of $N=20$ isotones. This indicates the disappearance of the magic number $N=20$ in these neutron-rich nuclei. In this paragraph, we focused on neutron magic number $N=20$. However, it is noted that the proton numbers $Z=14(^{34}\text{Si})$ and $Z=16(^{36}\text{S})$ show magic properties. These proton magic numbers are discussed in Ref. [16].

The disappearance of the magic numbers indicates a change of single-particle energy spectra and the disappearance of a large energy gap at $N=8$ and $N=20$ in neutron-rich nuclei. In the next section and later, we discuss the single-particle energies using the shell-model sum rule and demonstrate the theoretical calculation for single-particle energies.

III. SINGLE-PARTICLE ENERGY

A. Spectroscopic definition of single-particle energy

The single-particle energy is well defined for a doubly closed shell nucleus. When a neutron is transferred to the core nucleus, the stripping reaction leads to a single state that carries the whole single-particle strength, as depicted in the left panel of Fig. 3. Then the single-particle energy is defined by the energy difference between the target core nucleus and the single-particle state. However, this is an ideal case. The transferred neutron would polarize the core. As a result, the single-particle strength is fragmented among several states. In such a case, the single-particle energy is defined as the center of gravity of the single-particle strengths,

$$\varepsilon_j = \textstyle\sum_f G_{fi}^{+j}\mathcal{E}_{fi}^{+j}. \tag{2}$$

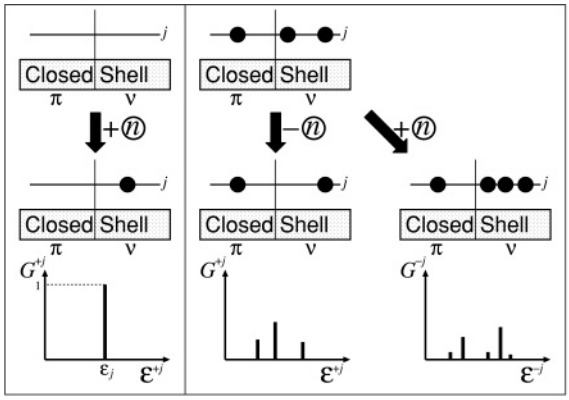

FIG. 3. Excitation energies of one-neutron transfer reactions for a closed-shell nucleus (left panel) and a open-shell nuclei (right panel).

Here, G_{fi}^{+j} and $\mathcal{E}_{fi}^{+j}$ are the single-particle strength and energy difference, respectively, of the final state f of the stripping reaction, and the sum of G_{fi}^{+j} is normalized to unity. Equation (2) has often been used for the evaluation of an empirical single-particle energy of a single-particle orbit j above the Fermi energy. Pick-up reaction on a doubly closed core state, in a similar way, populates states that share the strength of a single-particle orbit j below the Fermi energy, and then the single-particle energy is given by

$$\varepsilon_j = \sum_f G_{fi}^{-j} \mathcal{E}_{fi}^{-j}, \tag{3}$$

which corresponds to Eq. (2) for the stripping reaction.

For a target nucleus with valence nucleons, both stripping to and pick up from the same single-particle orbit j are possible, and the single-particle strength is fragmented among a number of final states of the transfer reactions (see the right panel of Fig. 3). Then, we can define the single-particle energy of the j orbit, according to French [26] and Baranger [27], by

$$\varepsilon_j = \sum_f G_{fi}^{+j} \mathcal{E}_{fi}^{+j} + \sum_f G_{fi}^{-j} \mathcal{E}_{fi}^{-j}, \tag{4}$$

generalizing the equations shown above for the closed-core state. $\mathcal{E}_{fi}^{+j}$ and $\mathcal{E}_{fi}^{-j}$ are excitation energies of the final states of the one-nucleon transfer reactions

$$\mathcal{E}_{fi}^{+j} = E_{n+1k_fJ_f} - E_{nk_iJ_i}, \tag{5}$$

$$\mathcal{E}_{fi}^{-j} = E_{nk_iJ_i} - E_{n-1k_fJ_f}, \tag{6}$$

where E_{nkJ} is the energy of the n-valence nucleon state $|nkJM\rangle$. The index k represents additional quantum numbers to distinguish wave functions with the same set of quantum numbers n, J, and M. The spectroscopic strengths are defined as

$$G_{fi}^{+j} = \frac{1}{[j]^2} \frac{[J_f]^2}{[J_i]^2} S_{fi}^{+j}, \tag{7}$$

$$G_{fi}^{-j} = \frac{1}{[j]^2} S_{fi}^{-j}, \tag{8}$$

where $[j]$ denotes $\sqrt{2j+1}$. S_{fi}^{+j} and S_{fi}^{-j} are spectroscopic factors of stripping and pick-up reactions [28], respectively, and they are defined as

$$S_{fi}^{+j} = \frac{1}{[J_f]^2} |\langle n+1k_fJ_f \| \hat{\boldsymbol{a}}_j^\dagger \| nk_iJ_i \rangle|^2, \tag{9}$$

$$S_{fi}^{-j} = \frac{1}{[J_i]^2} |\langle nk_iJ_i \| \hat{\boldsymbol{a}}_j^\dagger \| n-1k_fJ_f \rangle|^2, \tag{10}$$

where $\langle \cdot \| \cdot \| \cdot \rangle$ is a reduced matrix element. It is more convenient to use the spectroscopic strengths rather than the spectroscopic factors, since the spectroscopic strengths are given in the same form for both stripping and pickup,

$$G_{fi}^{+j} = \frac{1}{[j]^2} \sum_{M_f m} |\langle n+1k_fJ_fM_f | \hat{a}_{jm}^\dagger | nk_iJ_iM_i \rangle|^2, \tag{11}$$

$$G_{fi}^{-j} = \frac{1}{[j]^2} \sum_{M_f m} |\langle n-1k_fJ_fM_f | \hat{a}_{jm} | nk_iJ_iM_i \rangle|^2, \tag{12}$$

and the sum rules are given as

$$\sum_f G_{fi}^{+j} = 1 - \frac{n_j}{[j]^2}, \tag{13}$$

$$\sum_f G_{fi}^{-j} = \frac{n_j}{[j]^2}, \tag{14}$$

where n_j is the number of nucleons that occupy the single-particle orbit j. The right-hand side of Eq. (13) is the nonoccupation probability of the single-particle orbit j and that of Eq. (14) is the occupation probability of the single-particle orbit j. From Eqs. (13) and (14), we obtain the normalization

$$\sum_f G_{fi}^{+j} + \sum_f G_{fi}^{-j} = 1. \tag{15}$$

This relation holds for the same initial state $|nk_iJ_i\rangle$. The sum of f in the stripping reaction runs over $n+1$ particle states, and that in the pick-up reaction over $n-1$ particle states.

Equation (4) can be applied for a closed-shell target state, and it is reduced to Eq. (2) and Eq. (3) for stripping and pick-up reactions, respectively. The definition (4) has been used in an experimental determination of single-particle energies [29] where the single-particle energies for open-shell nuclei ^{20,22}Ne are determined from the experimental data of the stripping (d, n) [29] and pick-up $(d, {}^3\mathrm{He})$ [30–32] reactions on ^{20,22}Ne nuclei.

B. Sum rule of single-particle energy

A theoretical evaluation of single-particle energies according to Eq. (4) requires energy eigenvalues $E_{n\pm1k_fJ_f}$ and wave functions $|n\pm1k_fJ_f\rangle$ of all final states for both stripping and pick-up reactions. However, we can derive a sum rule with which we can calculate single-particle energies with only the initial-state wave function $|nk_iJ_i\rangle$.

The first term on the right-hand side of Eq. (4) is rewritten by substituting the expressions of excitation energies and

spectroscopic strengths, Eqs. (5) and (11), as

$$\begin{aligned}\sum_f G^{+j}_{fi}\mathcal{E}^{+j}_{fi} &= \sum_{k_f J_f}\frac{1}{[j]^2}\sum_{M_f m}|\langle n+1k_f J_f M_f|\hat{a}^\dagger_{jm}|nk_i J_i M_i\rangle|^2\\ &\quad\times\left(E_{n+1k_f J_f}-E_{nk_i J_i}\right)\\ &= \frac{1}{[j]^2}\sum_m\sum_{k_f J_f M_f}\\ &\quad\times\Big\{\langle nk_i J_i M_i|\hat{a}_{jm}E_{n+1k_f J_f}|n+1k_f J_f M_f\rangle\\ &\quad\times\langle n+1k_f J_f M_f|\hat{a}^\dagger_{jm}|nk_i J_i M_i\rangle\\ &\quad-\langle nk_i J_i M_i|E_{nk_i J_i}\hat{a}_{jm}|n+1k_f J_f M_f\rangle\\ &\quad\times\langle n+1k_f J_f M_f|\hat{a}^\dagger_{jm}|nk_i J_i M_i\rangle\Big\}. \end{aligned}\tag{16}$$

Using eigenvalue equations for the states $|n+1k_f J_f M_f\rangle$ and $\langle nk_i J_i M_i|$, and taking the sum over $n+1$ nucleon final states by closure, we obtain

$$\begin{aligned}\sum_f G^{+j}_{fi}\mathcal{E}^{+j}_{fi} &= \frac{1}{[j]^2}\sum_m\langle nk_i J_i M_i|\hat{a}_{jm}\hat{H}\,\hat{a}^\dagger_{jm}|nk_i J_i M_i\rangle\\ &\quad-\frac{1}{[j]^2}\sum_m\langle nk_i J_i M_i|\hat{H}\,\hat{a}_{jm}\hat{a}^\dagger_{jm}|nk_i J_i M_i\rangle. \end{aligned}\tag{17}$$

Two terms on the right-hand side are summarized by a commutator and we obtain

$$\sum_f G^{+j}_{fi}\mathcal{E}^{+j}_{fi} = \frac{1}{[j]^2}\langle nk_i J_i M_i|\sum_m[\hat{a}_{jm},\hat{H}]\hat{a}^\dagger_{jm}|nk_i J_i M_i\rangle.\tag{18}$$

Similarly, by using Eqs. (6) and (12), the second term on the right-hand side of Eq. (4) is rewritten as

$$\sum_f G^{-j}_{fi}\mathcal{E}^{-j}_{fi} = \frac{1}{[j]^2}\langle nk_i J_i M_i|\sum_m\hat{a}^\dagger_{jm}[\hat{a}_{jm},\hat{H}]|nk_i J_i M_i\rangle.\tag{19}$$

Substituting Eqs. (18) and (19) in Eq. (4), we can express the single-particle energy as an expectation value of an operator,

$$\varepsilon_j = \langle nk_i J_i M_i|\frac{1}{[j]^2}\sum_m\{[\hat{a}_{jm},\hat{H}],\hat{a}^\dagger_{jm}\}|nk_i J_i M_i\rangle.\tag{20}$$

Using Eq. (20), we can evaluate single-particle energies from the Hamiltonian $\hat{H}$ and the initial-state wave function.

IV. APPLICATION TO THE SHELL-MODEL HAMILTONIAN

In the previous section, an operator expression was derived for the sum-rule calculation of single-particle energies. To evaluate the commutator and anticommutator, the shell-model Hamiltonian is presented with creation and annihilation operators. It will be shown that the single-particle energies are given in terms of the monopole interaction.

The shell model usually assumes a core, which consists of closed shells for both proton and neutron systems, and the Hamiltonian is given by a sum of one-body and two-body terms,

$$\hat{H} = \hat{H}_0 + \hat{V},\tag{21}$$

where

$$\hat{H}_0 = \sum_{jm}\varepsilon^{\rm core}_j\hat{a}^\dagger_{jm}\hat{a}_{jm},\tag{22}$$

$$\hat{V} = \sum_{\alpha\bar{\alpha}JM}\langle 2\alpha|\hat{V}|2\bar{\alpha}\rangle_J\,\hat{A}^\dagger(2\alpha JM)\,\hat{A}(2\bar{\alpha}JM).\tag{23}$$

$\varepsilon^{\rm core}_j$ are single-particle energies with respect to the core. Two-particle matrix elements of an effective interaction are denoted by $\langle 2\alpha|\hat{V}|2\bar{\alpha}\rangle_J$, where α represents antisymmetrized and orthonormalized two-particle basis states. $\hat{A}^\dagger(2\alpha JM)$ and $\hat{A}(2\bar{\alpha}JM)$ are two-particle creation and annihilation operators and are given as

$$\begin{aligned}\hat{A}^\dagger(2\alpha JM) &= \frac{1}{\sqrt{2}}\sum_{j_1m_1}\sum_{j_2m_2}\langle j_1,\,j_2|\}2\alpha J\rangle\\ &\quad\times\langle j_1m_1\;j_2m_2|JM\rangle\hat{a}^\dagger_{j_1m_1}\hat{a}^\dagger_{j_2m_2}, \end{aligned}\tag{24}$$

$$\begin{aligned}\hat{A}(2\bar{\alpha}JM) &= \frac{1}{\sqrt{2}}\sum_{\bar{j}_1\bar{m}_1}\sum_{\bar{j}_2\bar{m}_2}\langle 2\bar{\alpha}J\{|\bar{j}_1,\,\bar{j}_2\rangle\\ &\quad\times\langle\bar{j}_1\bar{m}_1\bar{j}_2\bar{m}_2|JM\rangle\hat{a}_{\bar{j}_2\bar{m}_2}\hat{a}_{\bar{j}_1\bar{m}_1}, \end{aligned}\tag{25}$$

respectively. The coefficients of fractional parentage (cfp) $\langle\cdot,\cdot|\}\cdot\rangle$ and $\langle\cdot\{|\cdot,\cdot\rangle$ guarantee the antisymmetrization and orthonormalization of the two-particle states. We evaluate in the following the commutator and anticommutator of Eq. (20) for the one-body part and the two-body part, respectively.

The sum-rule operator for the one-body part $\hat{H}_0$ of the Hamiltonian is written as

$$\{[\hat{a}_{jm},\hat{H}_0],\hat{a}^\dagger_{jm}\} = \sum_{j'm'}\varepsilon^{\rm core}_{j'}\{[\hat{a}_{jm},\hat{a}^\dagger_{j'm'}\hat{a}_{j'm'}],\hat{a}^\dagger_{jm}\}.\tag{26}$$

The commutator and subsequent anticommutator result in

$$\{[\hat{a}_{jm},\hat{a}^\dagger_{j'm'}\hat{a}_{j'm'}],\hat{a}^\dagger_{jm}\} = \delta_{jj'}\delta_{mm'},\tag{27}$$

and the operator of the one-body part is written as

$$\frac{1}{[j]^2}\sum_m\{[\hat{a}_{jm},\hat{H}_0],\hat{a}^\dagger_{jm}\} = \varepsilon^{\rm core}_j,\tag{28}$$

which is a diagonal operator. Therefore, $\hat{H}_0$ gives the single-particle energy for the core. The two-body part (23) of the Hamiltonian is rewritten as

$$\begin{aligned}\hat{V} &= \frac{1}{2}\sum_{\alpha\bar{\alpha}J}\sum_{j_1j_2}\sum_{\bar{j}_1\bar{j}_2}\langle j_1,\,j_2|\}2\alpha J\rangle\\ &\quad\times\langle 2\alpha|\hat{V}|2\bar{\alpha}\rangle_J\langle 2\bar{\alpha}J\{|\,\bar{j}_1,\,\bar{j}_2\rangle\\ &\quad\times\sum_{m_1m_2\bar{m}_1\bar{m}_2M}\langle j_1m_1\;j_2m_2|JM\rangle\langle\bar{j}_1\bar{m}_1\bar{j}_2\bar{m}_2|JM\rangle\\ &\quad\times\hat{a}^\dagger_{j_1m_1}\hat{a}^\dagger_{j_2m_2}\hat{a}_{\bar{j}_2\bar{m}_2}\hat{a}_{\bar{j}_1\bar{m}_1}, \end{aligned}\tag{29}$$

where we have used Eqs. (24) and (25). The commutator and anticommutator yield four terms:

$$\begin{aligned}\{[\hat{a}_{jm}, \hat{a}^\dagger_{j_1m_1}\hat{a}^\dagger_{j_2m_2}\hat{a}_{\bar{j}_2\bar{m}_2}\hat{a}_{\bar{j}_1\bar{m}_1}], \hat{a}^\dagger_{jm}\} \\ = \delta_{jj_1}\delta_{mm_1}\delta_{j\bar{j}_1}\delta_{m\bar{m}_1}\hat{a}^\dagger_{j_2m_2}\hat{a}_{\bar{j}_2\bar{m}_2} \\ - \delta_{jj_1}\delta_{mm_1}\delta_{j\bar{j}_2}\delta_{m\bar{m}_2}\hat{a}^\dagger_{j_2m_2}\hat{a}_{\bar{j}_1\bar{m}_1} \\ - \delta_{jj_2}\delta_{mm_2}\delta_{j\bar{j}_1}\delta_{m\bar{m}_1}\hat{a}^\dagger_{j_1m_1}\hat{a}_{\bar{j}_2\bar{m}_2} \\ + \delta_{jj_2}\delta_{mm_2}\delta_{j\bar{j}_2}\delta_{m\bar{m}_2}\hat{a}^\dagger_{j_1m_1}\hat{a}_{\bar{j}_1\bar{m}_1}, \end{aligned} \tag{30}$$

which are all diagonal. Furthermore, because of the symmetry of the cfp,

$$\langle j_2, j_1 \| 2\alpha J\rangle = -(-1)^{j_1+j_2-J}\langle j_1, j_2 | \} 2\alpha J\rangle, \tag{31}$$

and that of Clebsch-Gordan coefficients, the four terms are summarized as

$$\frac{1}{[j]^2}\sum_m \{[\hat{a}_{jm}, \hat{V}], \hat{a}^\dagger_{jm}\} = \sum_{j'} \Delta\varepsilon_{jj'}\hat{N}_{j'}. \tag{32}$$

Here, we have introduced

$$\begin{aligned}\Delta\varepsilon_{jj'} = 2\sum_{\alpha\bar{\alpha}J}\frac{[J]^2}{[j]^2[j']^2} \\ \times \langle j, j' \| 2\alpha J\rangle\langle 2\alpha|\hat{V}|2\bar{\alpha}\rangle_J\langle 2\bar{\alpha}J\{\!| j, j'\rangle, \end{aligned} \tag{33}$$

which is called the monopole interaction [33,34], and

$$\hat{N}_{j'} = \sum_{m'}\hat{a}^\dagger_{j'm'}\hat{a}_{j'm'} \tag{34}$$

is the number operator. Therefore, the single-particle energy Eq. (20) is evaluated by

$$\varepsilon_j = \varepsilon_j^{\rm core} + \sum_{j'}\Delta\varepsilon_{jj'}\langle nk_iJ_iM_i|\hat{N}_{j'}|nk_iJ_iM_i\rangle, \tag{35}$$

where the matrix element $\langle nk_iJ_iM_i|\hat{N}_{j'}|nk_iJ_iM_i\rangle$ denotes the number of nucleons that occupy the orbit j'. The monopole interaction $\Delta\varepsilon_{jj'}$ gives contributions to ε_j per nucleon in the orbit j'. The first term of Eq. (35) consists of the kinetic energy and interactions with nucleons in the core. The second term arises from interactions with nucleons in the valence orbits.

For a further reduction of the monopole interaction, we have to specify two-nucleon basis states $|2\alpha JM\rangle$ by explicitly writing them with single-particle orbits as $|j_1j_2;JM\rangle$ or $|j_2j_1;JM\rangle = (-1)^{j_1+j_2-J}|j_1j_2;JM\rangle$. Since the cfp in Eq. (33) are given as

$$\langle j, j' \| j_1j_2; J\rangle = \begin{cases} \dfrac{1}{\sqrt{2}}\left(\delta_{jj_1}\delta_{j'j_2} - (-1)^{j+j'-J}\delta_{jj_2}\delta_{j'j_1}\right) & (j \neq j') \\ \dfrac{1-(-1)^{2j-J}}{2}\delta_{jj_1}\delta_{jj_2} & (j = j'), \end{cases} \tag{36}$$

the monopole interaction (33) is rewritten as

$$\Delta\varepsilon_{jj'} = \sum_J \frac{1-(-1)^{2j-J}\delta_{jj'}}{[j]^2[j']^2}[J]^2\langle jj'|\hat{V}|jj'\rangle_J. \tag{37}$$

Kronecker's delta $\delta_{jj'}$ takes into account different normalizations of two-nucleon states. Namely, $\delta_{jj'} = 1$ when two identical nucleons occupy the same orbit, and $\delta_{jj'} = 0$ otherwise.

The matrix elements of the two-body interaction can alternatively be written in the isospin formalism. Since two-neutron states and two-proton states always have isospin $T = 1$, the corresponding monopole interaction is written as

$$\Delta\varepsilon_{jj'} = \sum_J\left(1-(-1)^{2j-J}\delta_{jj'}\right)\frac{[J]^2}{[j]^2[j']^2}\langle jj'|\hat{V}|jj'\rangle_{T=1,J}. \tag{38}$$

The neutron-proton monopole interaction is given as

$$\Delta\varepsilon_{jj'} = \sum_{TJ}\frac{1-(-1)^{2j-J-T+1}\delta_{jj'}}{2}\frac{[J]^2}{[j]^2[j']^2}\langle jj'|\hat{V}|jj'\rangle_{TJ}. \tag{39}$$

In the case of $j = j'$, the matrix element $\langle j^2|\hat{V}|j^2\rangle_{TJ}$ vanishes for $J + T = 0$ because of antisymmetrization.

V. NUMERICAL RESULTS

A. Single-particle energies of *p*-shell nuclei

We have made a numerical calculation for nuclei with the proton number $2 \leqslant Z \leqslant 8$ and fixed neutron number $N = 8$ to investigate the disappearance mechanism of the neutron magic number $N = 8$. We calculate single-particle energies ε_j of five neutron orbits, $j = 0p_{3/2}, 0p_{1/2}, 0d_{5/2}, 0d$, and $1s_{1/2}$, for the ground state $|\psi\rangle$ of each nucleus by using the equation

$$\varepsilon_j = \varepsilon_j^{\rm core} + \sum_{j'}\Delta\varepsilon_{jj'}\langle\psi|\hat{N}_{j'}|\psi\rangle, \tag{40}$$

where the monopole interaction $\Delta\varepsilon_{jj'}$ is defined by Eq. (37). The ground-state wave functions $|\psi\rangle$ are constructed in the p-shell model space. Namely, the inert ^{4}He core is assumed, $Z-2$ protons occupy the proton p-shell orbits, and the neutron p-shell orbits are fully occupied. We take the Cohen-Kurath (8–16) POT [35] for the p-shell interaction, including the single-particle energies $\varepsilon_j^{\rm core}$ for $j = 0p_{3/2}$ and $0p_{1/2}$. Single-particle energies of the sd-shell orbits for the ^{16}O core are taken from the Wildenthal USD interaction [36], and then $\varepsilon_j^{\rm core}$ with respect to the ^{4}He core are calculated by applying Eq. (40) to the doubly closed ground state of ^{16}O,

$$\varepsilon_j(^{16}\text{O core}) = \varepsilon_j(^4\text{He core}) + \sum_{j'}[j']^2\,\Delta\varepsilon_{jj'}. \tag{41}$$

The left-hand side is provided by the USD interaction, and the second term of the right-hand side is calculated with the Millener-Kurath interaction [37] as the p-sd intershell interaction.

In the present calculation of p-shell nuclei, which have no nucleons in the sd shell, the sum in Eq. (40) runs over $j' = 0p_{3/2}$ or $0p_{1/2}$ orbits. For the $0p_{3/2}$ and $0p_{1/2}$ orbits, the two-body Cohen-Kurath interaction between the valence p-shell nucleons gives contributions to the single-particle energies ε_j via the monopole interaction $\Delta\varepsilon_{jj'}$. The single-particle energies of the sd-shell orbits are determined only by the Millener-Kurath interaction.

The calculated results are shown in Fig. 4. In the closed-shell nucleus ^{16}O with $Z = 8$, the single-particle

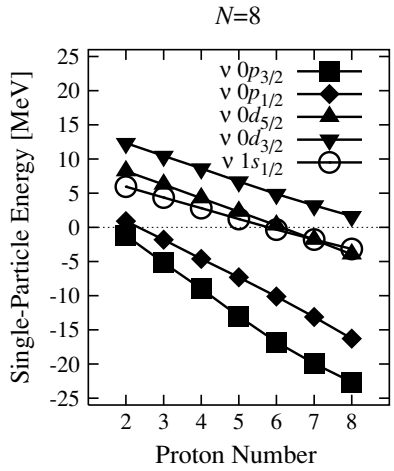

FIG. 4. Single-particle energies of neutron orbits for $N = 8$ isotones, calculated with the Cohen-Kurath (8–16) POT, the Millener-Kurath, and the Wildenthal USD interactions.

energies of the p-shell orbits are -22.646 MeV($0p_{3/2}$) and -16.283 MeV($0p_{1/2}$), which are determined by the Cohen-Kurath interaction, and those of the sd-shell orbits are -3.948 MeV($0d_{5/2}$), 1.647 MeV($0d_{3/2}$), and -3.164 MeV($1s_{1/2}$). In the neutron single-particle energy spectra, as protons are removed successively from $Z = 8$ to $Z = 2$, the energy gap between $1s_{1/2}$ and $0p_{1/2}$ decreases rapidly. The energy gap is 13.119 MeV at $Z = 8$ and 5.052 MeV at $Z = 2$. Of the two neutron orbits, $0p_{1/2}$ increases as the proton number decreases, whereas $1s_{1/2}$ stays rather constant [12,15]. The rapid increase of the former thus causes the disappearance of the large energy gap at the neutron $N = 8$ magic number. Because the calculation assumes the $0\hbar\omega$ model space with the interactions that were fitted to stable nuclei, it may not reproduce experimental data for halo nuclei, such as ^{11}Li and ^{12}Be, where mixing of excited configurations (i.e., $1\hbar\omega$ and $2\hbar\omega$ states) plays an important role. The mixing, however, is caused by the decrease of the energy gap between $1s_{1/2}$ and $0p_{1/2}$. An improved nuclear wave function with the excited configurations would yield a lower single-particle energy of $1s_{1/2}$, leading to a smaller gap, and give a better agreement with experiment.

We focus, in the following, on the single-particle energy of the neutron $0p_{1/2}$ orbit, since it plays the key role for the $N = 8$ energy gap. First, we show in Table I the contributions $\Delta\varepsilon_{jj'}$ from the p-shell orbits j' to the single-particle energies of the five neutron orbits. It is clear that the contributions from the neutron-proton interaction are large, and, in contrast, the neutron-neutron interaction gives almost no gain in single-particle energy. According to Eq. (37), the single-particle energy of neutron $0p_{1/2}$ decreases as protons occupy the $j' = 0p_{3/2}$ and $0p_{1/2}$ orbits with approximately constant slope, owing to the large negative, and almost equal, values of the neutron-proton monopole interactions shown in Table I. The neutron-proton monopole interactions $\Delta\varepsilon_{0p_{1/2},0p_{3/2}}$ and $\Delta\varepsilon_{0p_{1/2},0p_{1/2}}$ are about twice as large as $\Delta\varepsilon_{1s_{1/2},0p_{3/2}}$ and $\Delta\varepsilon_{1s_{1/2},0p_{1/2}}$. The differences of these values generate the large decrease of the energy gap between the $1s_{1/2}$ and $0p_{1/2}$ orbits.

TABLE I. Contributions $\Delta\varepsilon_{jj'}$ to ε_j of the neutron p- and sd-shell orbits from the p-shell orbits.

j	$\Delta\varepsilon_{jj'}$ (MeV)			
	neutron-proton		neutron-neutron	
	$j' = \pi 0p_{3/2}$	$j' = \pi 0p_{1/2}$	$j' = \nu 0p_{3/2}$	$j' = \nu 0p_{1/2}$
$\nu 0p_{3/2}$	-4.006	-2.718	-0.360	-0.439
$\nu 0p_{1/2}$	-2.718	-3.157	-0.439	0.120
$\nu 0d_{5/2}$	-1.971	-2.144	-0.449	-0.595
$\nu 0d_{3/2}$	-1.889	-1.565	-0.141	0.137
$\nu 1s_{1/2}$	-1.591	-1.378	-0.178	0.180

B. Single-particle energies of *sd*-shell nuclei

We have made a numerical calculations for nuclei with proton numbers $8 \leqslant Z \leqslant 20$ and fixed neutron numbers $N = 20$ and $N = 16$ to investigate the disappearance mechanism of the neutron magic number $N = 20$ and the existence of a new magic number $N = 16$. We calculate single-particle energies of seven neutron orbits, $0d_{5/2}$, $0d_{3/2}$, $1s_{1/2}$, $0f_{7/2}$, $0f_{5/2}$, $1p_{3/2}$, and $1p_{1/2}$, for the ground state of each nucleus. The ground-state wave functions $|\psi\rangle$ are constructed in the sd-shell model space with the inert ^{16}O core. We take the Wildenthal USD interaction [36] for the sd-shell interaction (i.e., the single-particle energies $\varepsilon_j^{\rm core}$ for $j = 0d_{5/2}, 0d_{3/2}$, and $1s_{1/2}$ with respect to the ^{16}O core and two-body interaction matrix elements). The USD interaction determines single-particle energies of the sd-shell orbits.

As the sd-fp intershell interaction, the Millener-Kurath interaction [37], which is usually used for the p-sd intershell interaction, is adopted by modifying the parameters as follows. The Millener-Kurath interaction is provided by Yukawa potentials, $V(r) = \exp(-r/\mu)/(r/\mu)$, where μ is a range parameter. Values of b/μ are given in Ref. [37] as $b/\mu = 1.18$ for the central and tensor parts and $b/\mu = 2.36$ for the spin-orbit part, where $b = \sqrt{\hbar/m\omega}$ is the b parameter of harmonic oscillator wave functions. We assume the Millener-Kurath interaction is given for $A = 16$ and that the range parameter is not changed in the $A = 16$–40 mass region. Using the formula [38] $\hbar\omega = 45A^{-1/3} - 25A^{-2/3}$ MeV, we evaluate the b parameters for the $A = 16$ and $A = 40$ cases, and we obtain $b^{(A=40)}/b^{(A=16)} = 1.12391$. This gives the modified parameters, $b/\mu = 1.32622$ (central or tensor parts) and 2.65243 (spin-orbit part) for $A = 40$. Single-particle energies of the fp-shell orbits for ^{40}Ca are taken from Ref. [39] [-8.36 MeV($0f_{7/2}$), -1.86 MeV($0f_{5/2}$), -6.26 MeV($1p_{3/2}$), and -4.46 MeV($1p_{1/2}$)], and then $\varepsilon_j^{\rm core}$ with respect to the ^{16}O core are calculated with the Millener-Kurath interaction with the modified parameters, and by applying Eq. (40) to the doubly closed ground state of ^{40}Ca. The single-particle energies of the fp-shell orbits are determined only by the Millener-Kurath interaction in the present calculation of sd-shell nuclei, which have no nucleons in the fp-shell.

The Wildenthal USD interaction has a mass dependence. For the mass-dependent Hamiltonian, we derive the single-particle energy, Eq. (35), approximately as follows. In the case

of an A-nucleon system, the mass-dependent Hamiltonian is denoted by $\hat{H}^{(A)}$. The Hamiltonian with the Wildenthal USD interaction is given as $\hat{H}^{(A)} = \hat{H}_0 + \hat{V}^{(A)}$. The one-body part $\hat{H}_0$ does not have mass dependence. The values of two-body matrix elements are given for $A = 18$ nuclei, and those for other values of A are obtained by multiplying these values by $(18/A)^{0.3}$, as $\hat{V}^{(A)} = (18/A)^{0.3}\hat{V}^{(18)}$. Then, we rewrite the two-body part of an $(A \pm 1)$-nucleon system as

$$\hat{V}^{(A\pm1)} = \hat{V}^{(A)} \pm 0.3\frac{1}{A}\hat{V}^{(A)} + \cdots. \tag{42}$$

We retain only the first term, since the higher order terms with $1/A$ are much smaller than the first term (the zeroth-order term).

The calculated results for $N = 20$ nuclei are shown in Fig. 5(a). In the closed-shell nucleus ^{40}Ca with $Z = 20$, the single-particle energies of the sd-shell orbits are -24.634 MeV($0d_{5/2}$), -17.230 MeV($0d_{3/2}$), and -19.976 MeV($1s_{1/2}$), and those of the fp shell are -8.360 MeV($0f_{7/2}$), -1.860 MeV($0f_{5/2}$), -6.260 MeV($1p_{3/2}$), and -4.460 MeV($1p_{1/2}$). In the neutron single-particle energy spectra, as protons are removed successively from $Z = 20$ to $Z = 8$, the energy gap between the sd-shell orbit and the fp-shell orbit decreases. For instance, the energy gap between $0d_{3/2}$ and $1p_{3/2}$ is 10.970 MeV at $Z = 20$ and it decreases to 5.036 MeV at $Z = 8$. The magnitude of decrease in this case is smaller than that in the $N = 8$ case.

The occupation probabilities of the proton orbits for ground states of $N = 20$ isotones are shown in Fig. 5(b). In the case of $N = 20$ isotones, we can see that each one-nucleon state is filled by a nucleon in turn, starting from the lowest energy state. As protons are added successively from $Z = 8$ to $Z = 20$, up to $Z = 14$, the occupation probability of the only $0d_{5/2}$ orbit increases. Then the single-particle energies of neutron $0d$ orbits decrease with a constant slope. The single-particle energy of the $1s_{1/2}$ orbit decreases more loosely than those of $0d$ orbits. In the case of the isotones with $Z = 14$ to $Z = 16$, the $0d_{5/2}$ orbit is filled by valence protons and the occupation probability of the $1s_{1/2}$ orbit increases. Then the single-particle energy of the $1s_{1/2}$ orbit decreases rapidly and those of $0d$ orbits decrease loosely. In the case of the isotones with $Z = 16$ to $Z = 20$, the $0d_{5/2}$ and $1s_{1/2}$ orbits are filled by valence protons and the occupation probability of the $0d_{3/2}$ orbit increases. Then the single-particle energies of neutron $0d$ orbits decrease with a constant slope and that of the $1s_{1/2}$ orbit decreases loosely. In the fp-shell orbits, the single-particle energies of $0f$ orbits decrease like the $0d$ orbits and those of $1p$ orbits decrease like the $1s$ orbit.

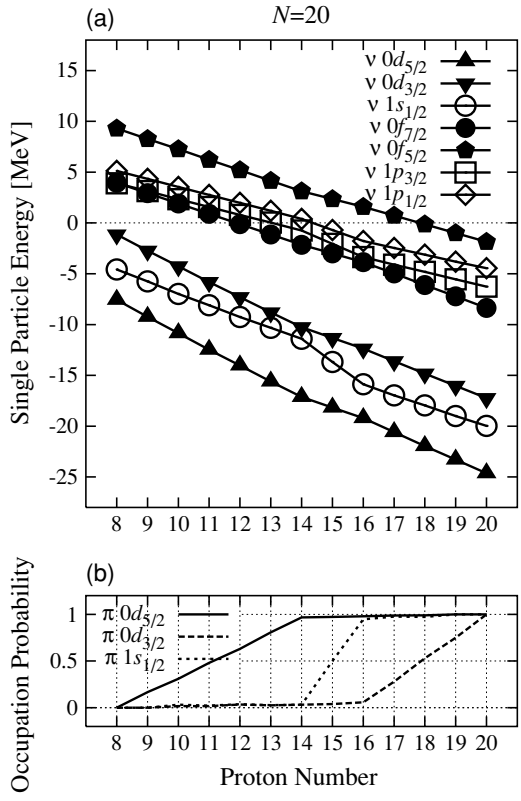

FIG. 5. Single-particle energies of neutron orbits (a) and occupation probabilities of proton orbits (b) for $N = 20$ isotones, calculated with the Wildenthal USD and the Millener-Kurath interactions.

The values of monopole interactions $\Delta\varepsilon_{jj'}$ are shown in Table II. A value of $A = 18$ is assumed for the mass-dependent USD interaction. The neutron-proton monopole interactions $\Delta\varepsilon_{0d,0d}$, $\Delta\varepsilon_{1s,1s}$, and $\Delta\varepsilon_{0d,1s}$ are larger than $\Delta\varepsilon_{0f,0d}$, $\Delta\varepsilon_{0f,1s}$, $\Delta\varepsilon_{1p,0d}$, and $\Delta\varepsilon_{1p,1s}$. This tendency is discussed by Schiffer and True [40], and we discuss it in Secs. VI B and VI E. When we focus on only the sd-shell orbits, the neutron-proton monopole interactions $\Delta\varepsilon_{0d,0d}$ and $\Delta\varepsilon_{1s,1s}$ are larger than $\Delta\varepsilon_{0d,1s}$. Similarly, in the neutron-proton monopole interactions between the sd-shell orbit and the fp-shell orbit, $\Delta\varepsilon_{0f,0f}$ and $\Delta\varepsilon_{1p,1p}$ are larger than $\Delta\varepsilon_{0f,1p}$. These tendency of the strengths of the monopole interactions is the same as the case of the p-shell nuclei given in Table I. In Fig. 5(a), the single-particle energies of $0d$ orbits decrease more rapidly than that of the $1s$ orbit at the $Z = 8$–14 and $Z = 16$–20 regions. Moreover, the single-particle energy of the $1s$ orbit decreases more rapidly than those of $0d$ orbits at the $Z = 14$–16 region. These strength differences of decreases of single-particle energies consist of neutron-proton monopole interactions. It seems that the monopole interaction between the orbits that have the same nodal quantum number is larger than that between orbits that have different nodal quantum numbers, and we discuss this in Sec. VI E.

TABLE II. Contributions $\Delta\varepsilon_{jj'}$ to ε_j of the neutron sd- and fp-shell orbits from the sd-shell orbits.

	$\Delta\varepsilon_{jj'}$ (MeV)					
j	neutron-proton			neutron-neutron		
	$\pi 0d_{5/2}$	$\pi 0d_{3/2}$	$\pi 1s_{1/2}$	$\nu 0d_{5/2}$	$\nu 0d_{3/2}$	$\nu 1s_{1/2}$
$\nu 0d_{5/2}$	−1.978	−1.884	−1.375	−0.517	−0.310	0.104
$\nu 0d_{3/2}$	−1.884	−1.684	−1.387	−0.310	−0.315	−0.027
$\nu 1s_{1/2}$	−1.375	−1.387	−2.978	0.104	−0.027	−1.062
$\nu 0f_{7/2}$	−1.015	−1.137	−0.834	−0.187	−0.293	−0.134
$\nu 0f_{5/2}$	−1.039	−0.859	−0.749	−0.120	0.031	−0.007
$\nu 1p_{3/2}$	−0.769	−0.707	−1.360	−0.068	0.048	−0.368
$\nu 1p_{1/2}$	−0.787	−0.653	−1.128	−0.076	0.102	0.113

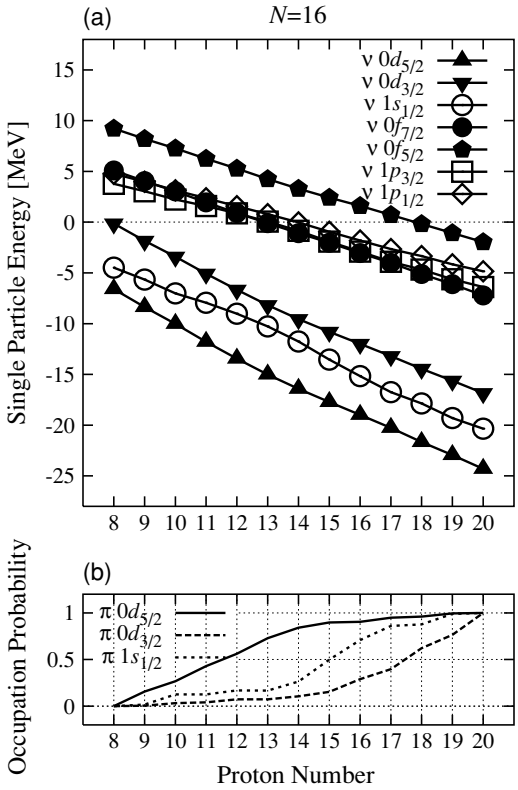

FIG. 6. Single-particle energies of neutron orbits (a) and occupation probabilities of proton orbits (b) for $N = 16$ isotones, calculated with the Wildenthal USD and the Millener-Kurath interactions.

The neutron single-particle energies of $N = 16$ isotones are shown in Fig. 6(a). The energy gap between sd-shell orbits and fp-shell orbits for the $N = 16$ case is narrower than that for the $N = 20$ case. For instance, the energy gap between $0d_{3/2}$ and $1p_{3/2}$ is 9.905 MeV at $Z = 20$ and 3.908 MeV at $Z = 8$. At the $Z < 13$ region, as protons are removed successively, the energy gap between $0d_{3/2}$ and $1s_{1/2}$ orbits becomes larger. The large energy gap between $0d_{3/2}$ and $1s_{1/2}$ orbits at $Z = 8$ suggests the appearance of magic number $N = 16$. This statement is made on empirical grounds by including fp and sdg shells besides p and sd shells in Refs. [16,41–43]. Moreover, since the neutron $0d_{3/2}$ single-particle energy is about 0 MeV at $Z = 8$, the neutron $0d_{3/2}$ single-particle state would be unstable. This numerical result is consistent with the experimental result that ^{25}O is not a bound system.

The occupation probabilities of proton orbits for ground states of $N = 16$ isotones are shown in Fig. 6(b). In the case of the $N = 16$ isotones, valence protons are contained also in the upper ($1s_{1/2}$ and $0d_{3/2}$) orbits although the lower ($0d_{5/2}$) orbit has not filled. Unlike the case of $N = 20$ isotones, it is thought the configuration mixing is large in the case of $N = 16$ isotones.

In Figs. 5 and 6, we have shown the theoretical calculations of single-particle energies. For open-shell nuclei, to determine the single-particle energies experimentally, we need experimental data of stripping and pick-up reactions, such as those in Ref. [29]. For closed-shell nuclei, we can evaluate single-particle energies from mass-excess data. Since ^{36}S nuclei ($Z = 16$ and $N = 20$) have doubly magic features [16], we obtain the energy gap $\Delta E^{\rm exp}$ between $\nu 0d_{3/2}$ and $\nu 0f_{7/2}$ orbits, $\Delta E^{\rm exp} = 5.585$ MeV, by using the following equation:

$$\Delta E^{\rm exp} = \varepsilon(\nu 0f_{7/2}) - \varepsilon(\nu 0d_{3/2}) = (\Delta(^{37}\mathrm{S}) - \Delta(^{36}\mathrm{S})) - (\Delta(^{36}\mathrm{S}) - \Delta(^{35}\mathrm{S})), \quad (43)$$

where $\Delta(^A\mathrm{S})$ denotes the mass excess of the S nucleus with mass number A, and the experimental values are $\Delta(^{35}\mathrm{S}) = -28.846$, $\Delta(^{36}\mathrm{S}) = -30.664$ and $\Delta(^{37}\mathrm{S}) = -26.896$ MeV, respectively [44]. In Fig. 5, the theoretical result of this energy gap is $\Delta E^{\rm theory} = 8.508$ MeV, which overestimates the experimental value of 5.585 MeV. Similarly, since ^{36}Ca nuclei ($Z = 20$ and $N = 16$) are the mirror nuclei for ^{36}S, we obtain the energy gap between $\nu 1s_{1/2}$ and $\nu 0d_{3/2}$ orbits, $\Delta E^{\rm exp} = 4.318$ MeV, by using the following equation:

$$\Delta E^{\rm exp} = \varepsilon(\nu 0d_{3/2}) - \varepsilon(\nu 1s_{1/2}) = (\Delta(^{37}\mathrm{Ca}) - \Delta(^{36}\mathrm{Ca})) - (\Delta(^{36}\mathrm{Ca}) - \Delta(^{35}\mathrm{Ca})), \quad (44)$$

where the experimental values of Δ are $\Delta(^{35}\mathrm{Ca}) = 4.600$, $\Delta(^{36}\mathrm{Ca}) = -6.440$, and $\Delta(^{37}\mathrm{Ca}) = -13.162$ MeV, respectively [44]. In Fig. 6, the theoretical result $\Delta E^{\rm theory} = 3.516$ MeV underestimates the experimental value of 4.318 MeV. In this study, excitations to the fp shell are not taken into account; that is, the model space consists of only the sd shell and the two-body matrix elements [36] are tuned for this model space. When we use the model space constructed by sd and fp shells and the appropriate two-body matrix elements for this model space, mixing of excited configurations would yield an upper single-particle energy of $0d_{3/2}$, leading to a smaller $0d_{3/2}$-$0f_{7/2}$ gap and a larger $1s_{1/2}$-$0d_{3/2}$ gap.

VI. DISCUSSION

A. Monopole interaction

The importance of the monopole interaction was first emphasized by Bansal and French [33]. They derived a simple equation for average energies of one-hole-many-particle states by introducing isoscalar and isovector monopole interactions. The isoscalar monopole is the same as in this study, whereas the isovector monopole gives rise to a shift of the average energy according to the isospin of the many-particle states to which the hole couples.

The monopole interaction often appears in nuclear structure calculations. We show some examples in the following. First, the energy of a core is a sum of monopole interactions, in addition to the kinetic energy contribution,

$$E = \sum_j E_j^{\rm kin} + \sum_{jj'} [j]^2 [j']^2 \Delta\varepsilon_{jj'}, \quad (45)$$

where the sum runs over all possible combinations of jj' in the core, including $j = j'$. The core is composed of closed shells with seniority $v = 0$ (i.e., all nucleons in the core are coupled pairwise to $J^\pi = 0^+$). This expression indicates that the binding energy of a core is determined only by the monopole, the J average of two-particle matrix elements of the two-body interaction.

A shell-model calculation uses single-particle energies, as a input, that are defined with respect to a core. When a core is raised to another core by filling nucleons, single-particle energies are changed accordingly. Denoting the lower and higher cores by core-1 and core-2, respectively, we can relate single-particle energies of the same j orbit with respect to the two cores by

$$\varepsilon_j^{\text{core-2}} = \varepsilon_j^{\text{core-1}} + \sum_{j'}[j']^2 \Delta\varepsilon_{jj'}, \tag{46}$$

where the sum of j' is taken for single-particle orbits that are out of core-1 but in core-2. This relation was given in many preceding studies, for example, the early Blomqvist-Rydström work [45] and, recently, the Grawe work [43]. In the previous section, the relation (46) has been used in the numerical calculations. It is noted that both cores are closed shells, and they have seniority $v = 0$.

The BCS ground state is described by a superposition of seniority $v = 0$ states by ansatz, to take into account the distribution of $J^\pi = 0^+$ pairs, owing to the pairing interaction, among various single-particle orbits. The distribution is determined by variation, with respect to u_j and v_j factors, which are amplitudes of the Bogoliubov transformation, by minimizing the expectation value of the Hamiltonian for the BCS ground state. Then, single-particle energies are given as $\varepsilon_j = \varepsilon_j^{\text{core}} + \mu_j$, where $\varepsilon_j^{\text{core}}$ denotes the single-particle energy with respect to the core and

$$\mu_j = \sum_{j'}[j']^2 v_{j'}^2 \Delta\varepsilon_{jj'} \tag{47}$$

contains interactions between nucleons outside the core. The monopole interaction appears, in the BCS calculation, always associated with v_j^2, the occupation probability in the single-particle orbit j. This corresponds to the number operator in the sum-rule expression derived in Sec. IV.

The monopole interaction has thus been used for single-particle energies for seniority $v = 0$ state; the closed shells in the shell model and the states with $J^\pi = 0^+$ pairs in BCS calculations. However, the sum rule of the present study can apply not only to closed shells but also to open-shell nuclei with unpaired nucleons. Furthermore, single-particle energies given by the sum rule are state dependent even in the same nucleus, as they should be.

Another important issue concerning the monopole interaction is that interactions designed by effective interaction theories in many-body systems, such as the G-matrix effective interaction, do not reproduce experimental single-particle energy spectra [34]. The source of disagreements is found in the monopole part of those effective interactions and these disagreements are known as the monopole problem. Most shell-model calculations have, therefore, employed phenomenological effective interactions, such as the Cohen-Kurath interaction [35] and the Wildenthal USD interaction [36], which were determined so as to reproduce experimental level energies. For the same reason, in BCS calculations, we do not evaluate μ_j, and instead we take, for example, eigenvalues of a Woods-Saxon potential for the sum $\varepsilon_j^{\text{core}} + \mu_j$.

Using the G-matrix formalism [46,47], effective interactions have been calculated from bare potentials of free NN scattering, such as the Reid potential [48], the Paris potential [49], the Bonn potential [50], and the Nijmegen potential [51]. However, the effective interactions obtained using the ordinary numerical G-matrix method have weak monopole interaction and need correction. In ordinary numerical G-matrix calculations, the effects of the three-body force and of higher energy states are considered as causes of the weak monopole interaction. For the effect of the three-body force, Zuker *et al*. reproduced the experimental level energies by a monopole correction [52] and Zuker suggested that the three-body force plays an important role for the monopole correction [53]. The monopole problem and the three-body force are explained in Ref. [54]. With respect to the effects of higher energy states, renormalization of high-momentum components may not be sufficient enough in low-momentum effective interaction in the truncated model space. In the unitary model operator approach (UMOA) [55], much effort has been devoted to the efficient treatment of short-range correlations, and, as a result, the monopole interaction has been improved.

B. Decomposition of the monopole interaction

One of the purposes of this study is to clarify the mechanism that causes the change of the neutron single-particle spectrum, when protons are removed from a nucleus. For that purpose, it is important to analyze contributions of various components of the two-body interactions to the single-particle energies. It will be shown that the triplet-even central interaction plays a decisive role for the monopole for all the effective interactions that are employed in the numerical calculations.

Here we suppose that a two-body interaction $\hat{V}$ consists of central (C), spin-orbit (LS), and tensor (TN) forces,

$$\hat{V} = \hat{V}_C + \hat{V}_{LS} + \hat{V}_{TN}. \tag{48}$$

Interaction channels are classified by total spin S, total isospin T, and the parity of orbital angular momentum L of two-nucleon states. Because of the condition $L + S + T =$ odd derived from the antisymmetrization of two-nucleon states, the channels are restricted to singlet-odd (SO), triplet-even (TE), singlet-even (SE), and triplet-odd (TO). The central force $\hat{V}_C$ can be written as

$$\begin{aligned}\hat{V}_C = {} & V_{\text{SO}}(r)\hat{\Pi}_\sigma^{\text{S}}\hat{\Pi}_\tau^{\text{S}} + V_{\text{TE}}(r)\hat{\Pi}_\sigma^{\text{T}}\hat{\Pi}_\tau^{\text{S}} \\ & + V_{\text{SE}}(r)\hat{\Pi}_\sigma^{\text{S}}\hat{\Pi}_\tau^{\text{T}} + V_{\text{TO}}(r)\hat{\Pi}_\sigma^{\text{T}}\hat{\Pi}_\tau^{\text{T}},\end{aligned} \tag{49}$$

where

$$\hat{\Pi}_\sigma^{\text{S}} = \frac{1 - \hat{\boldsymbol{\sigma}}_1 \cdot \hat{\boldsymbol{\sigma}}_2}{4}, \quad \hat{\Pi}_\sigma^{\text{T}} = \frac{3 + \hat{\boldsymbol{\sigma}}_1 \cdot \hat{\boldsymbol{\sigma}}_2}{4}, \tag{50}$$

$$\hat{\Pi}_\tau^{\text{S}} = \frac{1 - \hat{\boldsymbol{\tau}}_1 \cdot \hat{\boldsymbol{\tau}}_2}{4}, \quad \hat{\Pi}_\tau^{\text{T}} = \frac{3 + \hat{\boldsymbol{\tau}}_1 \cdot \hat{\boldsymbol{\tau}}_2}{4} \tag{51}$$

project onto spin/isospin singlet (S) and triplet (T) parts of the two-particle wave function. The spin-orbit force $\hat{V}_{\text{LS}}$ and the tensor force $\hat{V}_{\text{TN}}$ survive only between spin-triplet states and, therefore, have two components,

$$\hat{V}_{\text{LS}} = V_{\text{LSE}}(r)(\hat{\boldsymbol{L}} \cdot \hat{\boldsymbol{S}})\hat{\Pi}_\tau^{\text{S}} + V_{\text{LSO}}(r)(\hat{\boldsymbol{L}} \cdot \hat{\boldsymbol{S}})\hat{\Pi}_\tau^{\text{T}}, \tag{52}$$

$$\hat{V}_{\text{TN}} = V_{\text{TNE}}(r)\,\hat{S}_{12}\,\hat{\Pi}_\tau^{\text{S}} + V_{\text{TNO}}(r)\hat{S}_{12}\hat{\Pi}_\tau^{\text{T}}, \tag{53}$$

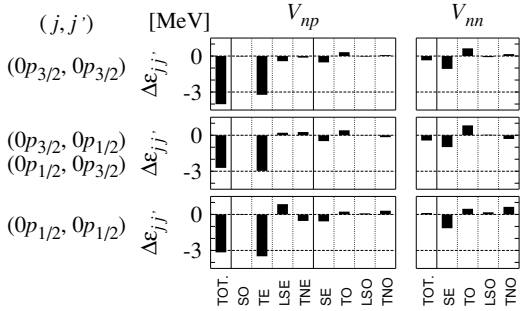

FIG. 7. Decomposition of the monopole interaction $\Delta\varepsilon_{jj'}$ into eight components of the Cohen-Kurath (8–16) POT interaction. $V_{np}(V_{nn})$ denotes the neutron-proton (neutron-neutron) interaction.

where $\hat{\boldsymbol{S}} = (\hat{\boldsymbol{\sigma}}_1 + \hat{\boldsymbol{\sigma}}_2)/2$ is the total spin operator of two-nucleon systems, $\hat{\boldsymbol{L}}$ is the relative orbital angular momentum operator, and

$$\hat{S}_{12} = \left(\frac{\hat{\boldsymbol{r}}}{r} \cdot \hat{\boldsymbol{\sigma}}_1\right)\left(\frac{\hat{\boldsymbol{r}}}{r} \cdot \hat{\boldsymbol{\sigma}}_2\right) - \frac{1}{3}(\hat{\boldsymbol{\sigma}}_1 \cdot \hat{\boldsymbol{\sigma}}_2) \tag{54}$$

is a scalar product of spatial and spin rank-two tensor operators. The radial potential $V_X(r)$ is a function of the distance r between two interacting nucleons.

In many cases of numerical calculations of nuclear structure, empirical interactions such as those of Refs. 70 [35,36] have been used. Matrix elements of the empirical interaction, which are given in the jj-coupling isospin formalism, $\langle jj'|\hat{V}|\bar{j}\bar{j}'\rangle_{TJ}$, are treated as free parameters and are determined by a least-squares fit to reproduce experimental level energies of various nuclei in a finite model space. Namely, no radial shapes are assumed for the potentials $V_X(r)$ and single-particle wave functions. However, we can decompose the matrix elements into components of the central, spin-orbit, and tensor forces by making use of tensorial structure of the forces. The procedure of decomposition is described in Ref. [35] for the p-shell empirical interaction, and we summarize the outline in Appendix A.

According to this procedure, we have decomposed the monopole interaction $\Delta\varepsilon_{jj'}$ into contributions from various components of the NN interaction. The decompositions for the p-shell orbits are shown in Fig. 7. They are calculated from fifteen two-particle matrix elements $\langle j_1 j_2|\hat{V}|\bar{j}_1\bar{j}_2\rangle_{TJ}$ of the Cohen-Kurath (8–16) POT interaction, which does not have an antisymmetric spin-orbit force. For all combinations of j and j', the triplet-even component in the $T = 0$ channel dominates $\Delta\varepsilon_{jj'}$. The triplet-even component is about -3 MeV. The same conclusion is obtained for the (8–16) 2BME and (6–16) 2BME sets of the Cohen-Kurath interaction [35]. This is traced to the strongly attractive interaction in the relative-S and spin-triplet state, which has the same quantum numbers as the deuteron (with a small D-state admixture). In the neutron-neutron interaction ($T = 1$), the contributions of the singlet-even channel and the triplet-odd channel are about 1 MeV. However, these contributions cancel each other to a large extent, and as a result, $\Delta\varepsilon_{jj'}$ becomes small.

The importance of the triplet-even attraction is not surprising and seems to be very reasonable from the viewpoint of nuclear binding. In a Hartree-Fock calculation, the nuclear binding energy, except for the kinetic energy term, is a sum of $[j]^2[j']^2\Delta\varepsilon_{jj'}$ over occupied single-particle orbits j and j'. A bound system is realized mainly by the attraction of the neutron-proton interaction. Furthermore, the success of Skyrme Hartree-Fock calculations with contact forces indicates the importance of the interaction in the relative S wave.

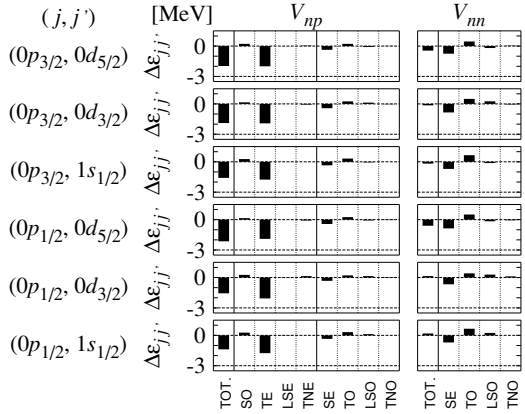

FIG. 8. Decomposition of the monopole interaction $\Delta\varepsilon_{jj'}$ into eight components of the Millener-Kurath interaction. $V_{np}(V_{nn})$ denotes the neutron-proton (neutron-neutron) interaction.

Figure 8 shows the decompositions of $\Delta\varepsilon_{jj'}$ of the Millener-Kurath p-sd intershell interaction, where j takes $0p_{3/2}$ or $0p_{1/2}$ and j' takes $0d_{5/2}$, $0d_{3/2}$, or $1s_{1/2}$. The Millener-Kurath interaction is provided by potentials, and we can directly calculate matrix elements of each component. We have used oscillator radial wave functions with $b/\mu = 1.18$ from Ref. [37], where b is a b parameter and μ is a range parameter. As in the case of the Cohen-Kurath interaction, the triplet-even component in the $T = 0$ channel dominates $\Delta\varepsilon_{jj'}$.

The decompositions of $\Delta\varepsilon_{jj'}$ for the sd-shell orbits are shown in Fig. 9. Nonzero matrix elements with $S \neq \bar{S}$ are obtained, which indicates antisymmetric spin-orbit forces in the Wildenthal interaction. However, the antisymmetric forces

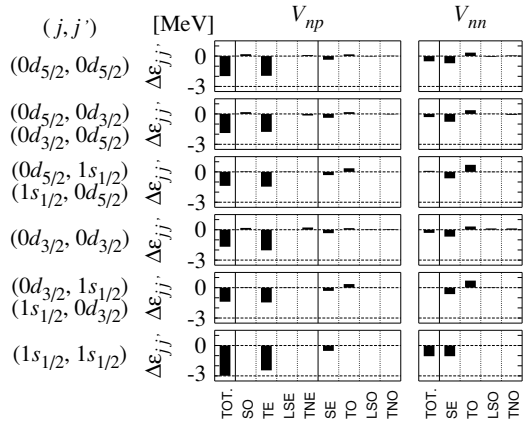

FIG. 9. Decomposition of the monopole interaction $\Delta\varepsilon_{jj'}$ into eight components of the Wildenthal USD interaction ($A = 18$). $V_{np}(V_{nn})$ denotes the neutron-proton (neutron-neutron) interaction.

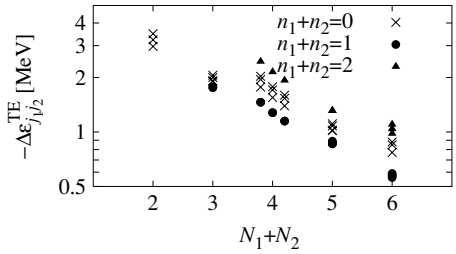

FIG. 10. The triplet-even channel of monopole interaction plotted against $N_1 + N_2$, where $N = 2n + \ell$. The crosses represent $n_1 + n_2 = 0$, the circles $n_1 + n_2 = 1$, and the triangles $n_1 + n_2 = 2$ multiplets.

TABLE III. The effective interactions used in to obtain the result of Fig. 10.

$N_1 + N_2$	Shell	Interaction	Ref.
2	p	Cohen-Kurath (8–16) POT	[35]
3	p-sd	Millener-Kurath	[37]
4	sd	Wildenthal USD (left: $A = 18$, center: $A = 28$, right: $A = 40$)	[36]
5	sd-fp	Millener-Kurath (modified such as in Sec. V B)	[37]
6	fp	Kuo-Brown	[46]

are weak and are omitted in Fig. 9. For all combinations of j and j', the triplet-even component in the $T = 0$ channel dominates $\Delta\varepsilon_{jj'}$. This conclusion is the same with the Cohen-Kurath interaction and the Millener-Kurath interaction. The triplet-even component is about -2 MeV.

The $1s_{1/2}$-$1s_{1/2}$ monopole interaction has a special feature. It has only two interaction channels, TE and SE, for the neutron-proton interaction. The former gives the largest negative value among $\Delta\varepsilon_{jj'}$ in the sd-shell orbits, and the latter enhances the attractive $1s_{1/2}$-$1s_{1/2}$ monopole. The $\nu 1s_{1/2} - \nu 1s_{1/2}$ monopole interaction takes a rather large value because there is no triplet-odd contribution, which cancels the singlet-even value to a certain extent in the other combinations. This special feature gives the large decrease of neutron $1s_{1/2}$ single-particle energy at the $Z = 14$–16 region, which is shown in Fig. 5 of Sec. V B.

In this section, we have pointed out the importance of the triplet-even component in the monopole interaction. Here, we show that the size of the triplet-even component of the monopole interaction depends on the quantum numbers N, n, and ℓ, where n is the nodal quantum number, ℓ denotes the orbital angular momentum, and $N = 2n + \ell$ determines a shell. Schiffer and True discussed the trends in the monopole interaction [40]. They studied the average size of matrix elements of NN interactions that were determined from experimental data and plotted the monopole interaction as a function of the sum $N_1 + N_2$ for the two orbits. In Fig. 10, the triplet-even components of the monopole interaction, $-\Delta\varepsilon^{\rm TE}_{j_1j_2}$, are plotted as a function of $N_1 + N_2$, such as was done in Ref. [40]. We take the effective interactions listed in Table III and calculate the monopole interaction. At $N_1 + N_2 = 4$, which corresponds to the sd-shell region, we plot three sets of data, $A = 18$ (left), $A = 28$ (center), and $A = 40$ (right), since the Wildenthal USD interaction has a mass dependence. The values of the triplet-even component of the monopole interaction, $|\Delta\varepsilon^{\rm TE}_{j_1j_2}| = -\Delta\varepsilon^{\rm TE}_{j_1j_2}$, decrease as $N_1 + N_2$ increases for $n_1 + n_2 = 0$, 1, and 2 cases, respectively. Also, the monopole interactions for the $n_1 + n_2 = 1$ cases, that is, $(n_1, n_2) = (1, 0)$ or $(0, 1)$, are smaller than those of $(n_1, n_2) = (0, 0)$ or $(2, 2)$ cases. This result suggests that the monopole interaction between the orbits that have the same nodal quantum number is larger than that between those with different nodal quantum numbers, and we discuss this in Sec. VI D.

C. Origin of the triplet-even attraction

In the bare NN interactions, the SE central channel has the strongest attractive potential. However, the effective interactions yield the dominant attractive contribution through the TE channel. The mechanism by which the effective TE channel obtains the strong attraction is discussed in Refs. [56,57]. Here, we demonstrate this mechanism for the two-nucleon system and discuss the important role of the tensor force, which arises mainly from one-pion exchange (OPE).

Among the four central channels, SE has the strongest attractive potential, as shown in the left figure of Fig. 11 [48]. However, the $^1S_0$ states of pp, nn, and pn ($T = 1$) systems are unbound. The two-nucleon bound state appears only in the TE channel, the deuteron, in spite of its weaker potential than that of the SE channel. The deuteron has the following quantum numbers: isospin $T = 0$, total angular momentum $J = 1$, and spin angular momentum $S = 1$. There is a mixture of $^3S_1$ and $^3D_1$ in the triplet-even channel with $J = 1$. Experiments on the magnetic moment and the quadrupole moment suggest that the deuteron state contains the $^3D_1$ component. Especially, the nonvanishing quadrupole moment arises only from the D component, since the S component is spherically symmetric.

The deuteron wave function can be written as a superposition of $^3S_1$ and $^3D_1$ components,

$$\psi = \frac{u(r)}{r}\left|{}^3S_1\right\rangle + \frac{w(r)}{r}\left|{}^3D_1\right\rangle. \tag{55}$$

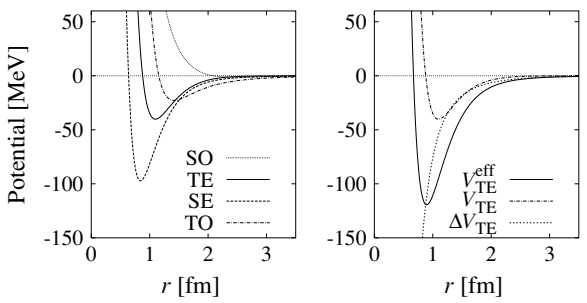

FIG. 11. The central potentials of the four channels in the Reid soft-core potential [48] (left). The effective potential of the TE channel (right).

The radial wave functions $u(r)$ and $w(r)$, which are normalized by

$$\int_0^\infty dr\,[u^2(r)+w^2(r)]=1, \tag{56}$$

are solutions of coupled eigenvalue equations,

$$\left(-\frac{\hbar^2}{m}\frac{d^2}{dr^2}+V_{\rm TE}(r)\right)u(r)+\sqrt{8}V_{\rm TNE}(r)w(r)=Eu(r), \tag{57}$$

$$\left(-\frac{\hbar^2}{m}\frac{d^2}{dr^2}+\frac{6\hbar^2}{mr^2}+V_{\rm TE}(r)-2V_{\rm TNE}(r)-3V_{\rm LSE}(r)\right)w(r)$$
$$+\sqrt{8}V_{\rm TNE}(r)u(r)=Ew(r), \tag{58}$$

where m is the nucleon mass. Since the ${}^3S_1$ and ${}^3D_1$ components cannot be coupled by the central force, the tensor force is indispensable for the coupling. In the region where the D-state component $w(r)$ is not vanishing, $V_{\rm TNE}(r)w(r)$ serves as a source term for the S-state component $u(r)$. If this term is regarded as a potential for the ${}^3S_1$ component,

$$\Delta V_{\rm TE}(r)=\sqrt{8}V_{\rm TNE}(r)w(r)/u(r), \tag{59}$$

it is as attractive as the central potential $V_{\rm TE}(r)$ in the range $r=$ 1–3 fm. With the help of the potential $\Delta V_{\rm TE}(r)$, the effective potential

$$V_{\rm TE}^{\rm eff}(r)=V_{\rm TE}(r)+\Delta V_{\rm TE}(r) \tag{60}$$

is more attractive than the SE central potential, as shown in right figure of Fig. 11, and the deuteron can exist as a bound state. The tensor potential $V_{\rm TNE}(r)$ arises mainly from the OPE.

Two nucleons in a nucleus interact mainly in the relative states with the lowest orbital angular momentum because of the centrifugal force. It is ${}^3S_1$ in the triplet-even channel, and there we have to consider the ${}^3S_1+{}^3D_1$ mixing, as we have discussed in the case of the deuteron. The mixing is illustrated in Fig. 12. The TE central potential is attraction in the medium range, and it is attributed to the exchange of the isoscalar-scalar σ in the meson exchange picture of nuclear forces. An effective central interaction that takes the effect of the tensor component generates a strong attractive potential in the TE channel. It is the part surrounded by the dashed line in the rightmost diagram in Fig. 12, where we suppose both initial and final states are ${}^3S_1$. The tensor component of the OPE potential generates a strong interaction between ${}^3S_1$ and ${}^3D_1$. The intermediate ${}^3D_1$ states in the dashed box are usually highly excited, sometimes

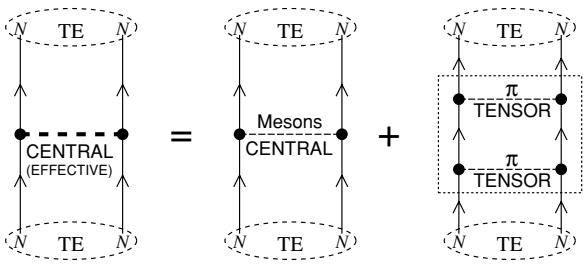

FIG. 12. An effective TE component of a one-pion exchange potential.

up to $10\hbar\omega$ excitation, since the tensor interaction of the OPE potential can induce transfers of high momenta.

Shell-model empirical interactions, such as the Cohen-Kurath interaction [35] and the Wildenthal interaction [36], are designed in a truncated model space, $p_{3/2}$-$p_{1/2}$ and $d_{5/2}$-$d_{3/2}$-$s_{1/2}$, respectively, and two-particle matrix elements are treated as free parameters in a least-squares fit calculation. In such a case, excitation to intermediate states outside the model space is renormalized in the optimized two-particle matrix elements. We understand that, in the TE channel, the effects of the OPE potential tensor interaction mentioned here are included in the central part of the shell-model effective interaction. Thus, the TE central component is strongly attractive partly because of the original central interaction and partly because of the second-order tensor correlations. By this mechanism, the central TE channel of the NN interaction becomes stronger than the SE channel. We note that the tensor force cannot affect the SE channel since this channel has $S=0$. The short-ranged SE potential is expected to contribute mainly to the pairing (i.e., the $J^\pi=0^+$ pair formation). But, the pairing matrix elements little affect the monopole interaction because of a small factor of $(2J+1)=1$ in the angular-momentum average of the monopole.

The importance of the tensor force has been emphasized in a phenomenon called the quenching of magnetic moments. In calculations of magnetic moments, we use orbital and spin g factors, according to the magnetic dipole interaction. The values of the g factors are $g_\ell=1\ \mu_N$, $g_s=5.58\ \mu_N$ for free protons and $g_\ell=0$ n.m., $g_s=-3.286$ n.m. for free neutrons, respectively. To reproduce experimental magnetic moments, we need to use, for most nuclei, $g_s^{\rm eff}=(0.7$–$0.8)g_s$. This is called the quenching of magnetic moments, or the quenching of the spin g factor. Shimizu, Ichimura, and Arima pointed out the importance of the tensor force [58]. They performed a second-order perturbation calculation and showed that magnetic moments of core $\pm$ one-nucleon systems are explained by the second-order tensor correlation. Large momentum transfer of the tensor interaction induces particle-hole excitations and a number of intermediate states with high excitation contribute to the magnetic moment in the ground state. Namely, excitation by the tensor interaction to intermediate states outside the model space is renormalized in the g factor with which magnetic moments are calculated in the truncated model space. Towner and Khanna discussed the importance of the tensor force for the quenching g factor of the Gamow-Teller β transitions in mirror nuclei [59,60]. They considered intermediate states up to $12\hbar\omega$ and their calculation was in good agreement with experiment.

Also, in the UMOA calculation, unperturbed harmonic oscillator energies up to about $20\hbar\omega$ are taken into account for the efficient treatment of the short-range part of the NN interaction, which contains the tensor force, and the numerical calculation results reproduce the experimental data for the ground-state properties of ^{16}O nuclei [61–63].

D. Spin-isospin component

Recently, Otsuka *et al*. discussed shell gaps in neutron-rich nuclei and suggested the importance of the neutron-proton

monopole interaction between spin-orbit partners, $j = \ell \pm 1/2$ [14]. In Ref. [64], Zuker commented their discussion quoting interesting examples of monopole drift [65,66]. Otsuka *et al.* showed a change of the single-particle energy of the neutron $0d_{3/2}$ orbit in going from ^{24}O to ^{30}Si. The nucleus ^{24}O has no proton on ^{16}O, and they assumed the pure $(\pi 0d_{5/2})^6$ configuration for ^{30}Si. Both nuclei have sixteen neutrons and closed orbits of $0d_{5/2}$ and $1s_{1/2}$ are assumed for neutrons. Otsuka *et al.* also calculated the $1s_{1/2}$-$0d_{3/2}$ gap in $N = 16$ isotones with three different effective interactions available in the *sd*-shell region, by assuming the lowest pure configuration for the protons outside the ^{16}O core.

Otsuka *et al.* suggested the importance of the central spin-isospin $(\hat{\boldsymbol{\sigma}}_1 \cdot \hat{\boldsymbol{\sigma}}_2)(\hat{\boldsymbol{\tau}}_1 \cdot \hat{\boldsymbol{\tau}}_2)$ component of the OPE potential for the shell gap [14]. The OPE potential consists of two components [i.e., a central $(\hat{\boldsymbol{\sigma}}_1 \cdot \hat{\boldsymbol{\sigma}}_2)(\hat{\boldsymbol{\tau}}_1 \cdot \hat{\boldsymbol{\tau}}_2)$ component and a tensor $(\hat{\boldsymbol{\tau}}_1 \cdot \hat{\boldsymbol{\tau}}_2)$ component],

$$\hat{V}^{\rm OPE} = \frac{f^2 \mu_\pi}{4\pi} \left\{ \frac{1}{3} V_{\rm C}^{\rm OPEP}(r)(\hat{\boldsymbol{\sigma}}_1 \cdot \hat{\boldsymbol{\sigma}}_2)(\hat{\boldsymbol{\tau}}_1 \cdot \hat{\boldsymbol{\tau}}_2) + V_{\rm TN}^{\rm OPE}(r)\, \hat{S}_{12}(\hat{\boldsymbol{\tau}}_1 \cdot \hat{\boldsymbol{\tau}}_2) \right\}, \tag{61}$$

$$V_{\rm C}^{\rm OPE}(r) = \frac{\exp(-\mu_\pi r)}{\mu_\pi r}, \tag{62}$$

$$V_{\rm TN}^{\rm OPE}(r) = \left(1 + \frac{3}{\mu_\pi r} + \frac{3}{(\mu_\pi r)^2}\right) \frac{\exp(-\mu_\pi r)}{\mu_\pi r}, \tag{63}$$

where f is a coupling constant, $\mu_\pi = m_\pi c/\hbar$ is the pion mass, and $\hat{S}_{12}$ is given by Eq. (54). By using the relations (50) and (51), $(\hat{\boldsymbol{\sigma}}_1 \cdot \hat{\boldsymbol{\sigma}}_2)$ and $(\hat{\boldsymbol{\tau}}_1 \cdot \hat{\boldsymbol{\tau}}_2)$ are written by the projection operators as

$$\hat{\boldsymbol{\sigma}}_1 \cdot \hat{\boldsymbol{\sigma}}_2 = -3\hat{\Pi}_\sigma^{\rm S} + \hat{\Pi}_\sigma^{\rm T}, \tag{64}$$

$$\hat{\boldsymbol{\tau}}_1 \cdot \hat{\boldsymbol{\tau}}_2 = -3\hat{\Pi}_\tau^{\rm S} + \hat{\Pi}_\tau^{\rm T}. \tag{65}$$

The central $(\hat{\boldsymbol{\sigma}}_1 \cdot \hat{\boldsymbol{\sigma}}_2)(\hat{\boldsymbol{\tau}}_1 \cdot \hat{\boldsymbol{\tau}}_2)$ component is written as

$$V_{\rm C}^{\rm OPE}(r)(\hat{\boldsymbol{\sigma}}_1 \cdot \hat{\boldsymbol{\sigma}}_2)(\hat{\boldsymbol{\tau}}_1 \cdot \hat{\boldsymbol{\tau}}_2) = V_{\rm C}^{\rm OPE}(r)\big(9\,\hat{\Pi}_\sigma^{\rm S}\hat{\Pi}_\tau^{\rm S} - 3\,\hat{\Pi}_\sigma^{\rm T}\hat{\Pi}_\tau^{\rm S} - 3\,\hat{\Pi}_\sigma^{\rm S}\hat{\Pi}_\tau^{\rm T} + \hat{\Pi}_\sigma^{\rm T}\hat{\Pi}_\tau^{\rm T}\big) \tag{66}$$

and, therefore, potentials of the TE, SO, SE, and TO channels are given as

$$V_{\rm SO}^{\rm OPE}(r) = 9V_{\rm C}^{\rm OPE}(r), \tag{67}$$

$$V_{\rm TE}^{\rm OPE}(r) = -3V_{\rm C}^{\rm OPE}(r), \tag{68}$$

$$V_{\rm SE}^{\rm OPE}(r) = -3V_{\rm C}^{\rm OPE}(r), \tag{69}$$

$$V_{\rm TO}^{\rm OPE}(r) = V_{\rm C}^{\rm OPE}(r). \tag{70}$$

The TE and SE channels have the same attractive potential and the SO channel has the strong repulsive potential. However, in the empirical interactions used in Sec. V, the monopole interaction of the TE channel is larger than that of the SE channel and the monopole interaction of the SO channel is much smaller. Therefore, the central $(\hat{\boldsymbol{\sigma}}_1 \cdot \hat{\boldsymbol{\sigma}}_2)(\hat{\boldsymbol{\tau}}_1 \cdot \hat{\boldsymbol{\tau}}_2)$ component cannot explain the empirical interaction and consequently the empirical shell gap. However, the tensor component of the OPE potential does play an important role. Because of the function $1 + 3/\mu_\pi r + 3/(\mu_\pi r)^2$, the tensor potential is much stronger than the central potential except for $\mu_\pi r \gg 1$. It enhances the TE attraction through the second-order contribution, in addition to the medium-range attraction from the exchange of an isoscalar scalar σ meson. In terms of the tensor force, Otsuka *et al.* have given a discussion of shell evolution in Refs. [67,68], which are follow-up papers of Ref. [14]. It is noted that they suggest the first-order contribution of tensor force, whereas the importance of the second-order contribution is suggested in this section.

E. Multipole expansion

In this section, we discuss contributions to $\Delta\varepsilon_{jj'}$ from components of the central force of the NN interaction, making use of the multipole expansion [69]. In Appendix B, we introduce the multipole expansion and apply it to the central force of the NN interaction. Here, it is convenient to use the spin/isospin representation

$$\hat{V} = V_0(r) + V_\sigma(r)(\hat{\boldsymbol{\sigma}}_1 \cdot \hat{\boldsymbol{\sigma}}_2) + V_\tau(r)(\hat{\boldsymbol{\tau}}_1 \cdot \hat{\boldsymbol{\tau}}_2) + V_{\sigma\tau}(r)(\hat{\boldsymbol{\sigma}}_1 \cdot \hat{\boldsymbol{\sigma}}_2)(\hat{\boldsymbol{\tau}}_1 \cdot \hat{\boldsymbol{\tau}}_2), \tag{71}$$

with $r = |\boldsymbol{r}_1 - \boldsymbol{r}_2|$. Each component is expressed as a sum of products of two one-body operators, one acting on the first nucleon and the other on the second nucleon. Since the nucleons are distinguished by the labeling, matrix elements of the *NN* interaction consist of direct and exchange terms,

$$\langle jj'|\hat{V}|jj'\rangle_{TJ} = \langle jj'|\hat{V}|jj'\rangle_{TJ}^{\rm direct} + \langle jj'|\hat{V}|jj'\rangle_{TJ}^{\rm exch}. \tag{72}$$

In the direct terms, spin-dependent central components do not contribute to the single-particle energies. This restriction is due to parity conservation and angular-momentum coupling of one-body operators and single-particle wave functions. Neglecting noncentral components, we obtain the direct term of the neutron-proton monopole interaction,

$$\Delta\varepsilon_{jj'}^{\rm direct} = \int_0^\infty p^2 dp [v_0(p) - v_\tau(p)] \phi_j(p)\, \phi_{j'}(p), \tag{73}$$

where p is the momentum transferred between the two nucleons, and $v_0(p)$ and $v_\tau(p)$ are the Fourier transforms of the radial potentials $V_0(r)$ and $V_\tau(r)$, respectively. $\phi_j(p)$ and $\phi_{j'}(p)$ are the form factors of single-particle states and are given as

$$\phi_j(p) = \langle j|j_0(pr_1)|j\rangle, \tag{74}$$

$$\phi_{j'}(p) = \langle j'|j_0(pr_2)|j'\rangle, \tag{75}$$

where $j_0(pr)$ is the spherical Bessel function of order zero, and the matrix elements of Eqs. (74) and (75) are integrated out with respect to $\boldsymbol{r}_1$ and $\boldsymbol{r}_2$, respectively.

The form factors $\phi_j(p)$ of single-particle states are shown in Fig. 13 as functions of p. Here we assume harmonic oscillator radial wave functions, and therefore spin-orbit partners, $j = \ell \pm 1/2$, have the same radial wave functions. The shapes of $\phi_{0p}(p)$, $\phi_{0d}(p)$, and $\phi_{0f}(p)$ are alike, and the shapes of $\phi_{1s}(p)$ and $\phi_{1p}(p)$ are alike. That is, the shapes of the wave functions with the same nodal quantum number are alike.

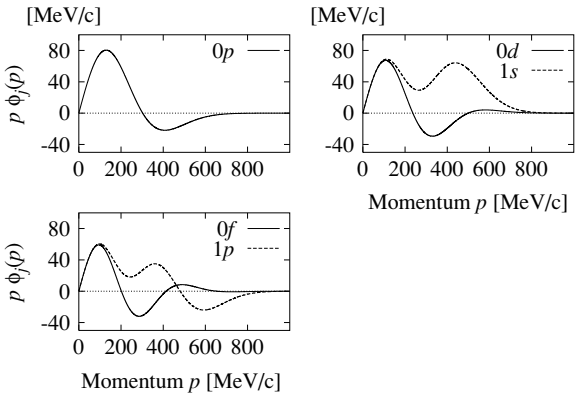

FIG. 13. The Fourier transforms of single-particle matrix elements as functions of p.

As an NN interaction, we consider a Dirac delta function $\delta(r)$ such as the Skyrme force. The Fourier-Bessel transform of $\delta(r)$ is a constant. Then, the direct term of the neutron-proton monopole interaction is evaluated as a overlap between $\phi_j(p)$ and $\phi_{j'}(p)$,

$$\Delta\varepsilon_{jj'}^{\text{direct}} = v_{\text{const}} \int_0^\infty p^2 dp\, \phi_j(p)\, \phi_{j'}(p). \tag{76}$$

Products of $\phi_j(p)$ and $\phi_{j'}(p)$ are shown in Fig. 14. The overlaps between the functions with the same nodal quantum number are larger than those with different nodal quantum numbers. Therefore, we expect large direct contributions for single-particle radial wave functions with a large overlap, such as between $j = \nu 0d_{3/2}$ and $j' = \pi 0d_{5/2}$. In contrast, a cancellation to a certain extent is expected for orbits with different nodal quantum numbers, such as $j = \nu 1s_{1/2}$ and $j' = \pi 0d_{5/2}$. In the monopole interactions $\Delta\varepsilon_{0d,0d}$, $\Delta\varepsilon_{1s,1s}$, and $\Delta\varepsilon_{0d,1s}$, which are calculated from the Wildenthal USD interaction, the relation between the strength of monopole interactions and the nodal quantum numbers is clear. The monopole interactions $\Delta\varepsilon_{0d,0d}$ and $\Delta\varepsilon_{1s,1s}$ have large values, whereas $\Delta\varepsilon_{0d,1s}$ has a smaller value. The Wildenthal USD interaction is an empirical interaction and no radial shapes are assumed for the potentials $V_X(r)$ and single-particle wave functions. However, it is considered that the $\Delta\varepsilon_{0d,0d}$ and

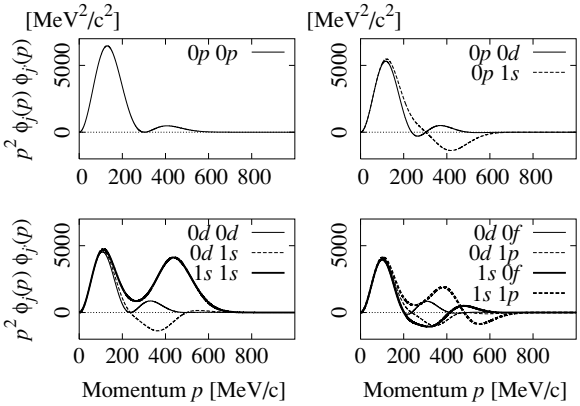

FIG. 14. Products of the Fourier transforms of single-particle matrix elements.

$\Delta\varepsilon_{1s,1s}$ have large overlaps between form factors with the same nodal quantum numbers, whereas $\Delta\varepsilon_{0d,1s}$ has a smaller overlap between those with different nodal quantum numbers.

Now, we consider the exchange term. Because of the spatial coordinate exchange between $\boldsymbol{r}_1$ and $\boldsymbol{r}_2$ of the particles, the multipole expansion for the exchange term gives a complicated form. In the case of $V(r) = V_{\text{const}}\delta(r)$, we can derive a simple form such as Eq. (73) for the direct term, and we obtain

$$\Delta\varepsilon_{jj'}^{\text{exch}} = \left(-v_\tau - 3v_{\sigma\tau}\right) \int_0^\infty p^2 dp\, \phi_j(p)\, \phi_{j'}(p), \tag{77}$$

where v_τ and $v_{\sigma\tau}$ are constants that are obtained by the Fourier-Bessel transformation of the δ functions. In the exchange term, only the isospin-dependent central components contribute to the neutron-proton monopole interaction. Generally, $V_0(r)$ and $V_\sigma(r)(\hat{\boldsymbol{\sigma}}_1 \cdot \hat{\boldsymbol{\sigma}}_2)$ do not contribute to the exchange term of neutron-proton monopole interaction for the following reason.

For $V(r) = V_{\text{const}}\delta(r)$, from the direct term [Eq. (73)] and exchange term [Eq. (77)], we obtain

$$\Delta\varepsilon_{jj'} = (v_0 - 2v_\tau - 3v_{\sigma\tau}) \int_0^\infty p^2 dp \phi_j(p)\, \phi_{j'}(p), \tag{78}$$

where v_0, v_τ, and $v_{\sigma\tau}$ are constants. Here, these constants are written as

$$v_0 = \frac{1}{16}(v_{\text{SO}} + 3v_{\text{TE}} + 3v_{\text{SE}} + 9v_{\text{TO}}), \tag{79}$$

$$v_\tau = \frac{1}{16}(-v_{\text{SO}} - 3v_{\text{TE}} + v_{\text{SE}} + 3v_{\text{TO}}), \tag{80}$$

$$v_{\sigma\tau} = \frac{1}{16}(v_{\text{SO}} - v_{\text{TE}} - v_{\text{SE}} + v_{\text{TO}}), \tag{81}$$

where v_{SO}, v_{TE}, v_{SE}, and v_{TO} are constants obtained by the Fourier-Bessel transformation of the δ functions for the SO, TE, SE, and TO channels. Therefore, we can rewrite Eq. (78) as

$$\Delta\varepsilon_{jj'} = \frac{3v_{\text{TE}} + v_{\text{SE}}}{4} \int_0^\infty p^2 dp\, \phi_j(p)\, \phi_{j'}(p). \tag{82}$$

In the case of the Dirac delta function potential, the triplet-even channel gives a large contribution to the monopole interaction. The approximation $V(r) = V_{\text{const}}\delta(r)$ is not so bad. It is shown in the success of Skyrme Hartree-Fock calculations with contact forces. The realistic wave functions and interaction generate the difference between the monopole interactions for the spin-orbit partners. But, from the calculation results in Sec. V, we expected that the difference would be small.

F. Proton single-particle energies

In the case of proton single-particle energies, we need to consider effects of the Coulomb force. Since the nuclear force is stronger than the Coulomb force at short range, the long-range part of the Coulomb force affects energies of nuclei. In a very rough argument, the Coulomb force is constant at long range. Then, only the diagonal part of the matrix elements of the Coulomb force has a nonzero value. Moreover, under the assumption that the Coulomb force is constant, contributions of the Coulomb force to all states are the same.

TABLE IV. The mass shifts $b^{\rm exp}(\alpha, T)$ and $c^{\rm exp}(\alpha, T)$ [MeV] for $A = 20$ nuclei [71].

	$T = 1$				$T = 2$
	$J^\pi = 1^+$	$J^\pi = 2^+$	$J^\pi = 3^+$	$J^\pi = 4^+$	0^+
$b^{\rm exp}$	4.162(8)	4.211(5)	4.179(10)	4.184(8)	4.224(4)
$c^{\rm exp}$	0.203(3)	0.186(6)	0.198(10)	0.163(8)	0.248(3)

It is shown that this assumption is not so bad by estimating the effects of the Coulomb force from mass differences among members of the isospin multiplet. The masses of members of an isospin multiplet can be described by the isospin-multiplet mass equation [70],

$$E(\alpha, T, T_z) = a(\alpha, T) + b(\alpha, T)T_z + c(\alpha, T)T_z^2, \quad (83)$$

where $E(\alpha, T, T_z)$ represents the mass of the member of the isospin multiplet, and α represents the quantum numbers except for the isospin T and its z-component T_z. Equation (83) is obtained by the Coulomb force operator $\sum_{ij} \hat{V}_{ij} \hat{\Pi}_i^p \hat{\Pi}_j^p$, where $\hat{V}_{ij}$ is the two-body operator that acts on an ordinary space, and $\hat{\Pi}^p = (\hat{1} - \hat{\tau}_z)/2$ is the projection operator that projects onto proton states. In Eq. (83), $b(\alpha, T)$ denotes the isovector mass shift and $c(\alpha, T)$ denotes the isotensor mass shift. Experimental mass shifts $b^{\rm exp}(\alpha, T)$ and $c^{\rm exp}(\alpha, T)$ are deduced in Ref. [71]. In Table IV, we show the mass shifts for $A = 20$ nuclei, which are obtained in Ref. [71]. The mass shifts are almost independent of J and T in the same mass nuclei. Namely, contributions from the Coulomb force are almost constant for states in the same mass nuclei. Therefore, the Coulomb force shifts the proton single-particle energies by a constant.

VII. CONCLUSION

The purpose of this study has been to investigate the mechanism of the change of neutron single-particle energy spectra with proton number in the p- and sd-shell regions by analyzing contributions of different components of NN interactions to the single-particle energy.

The single-particle energy has been defined as the center of gravity of the single-particle strengths. Using the shell-model sum rule for this definition, we have derived that the single-particle energy is written by the monopole interactions that give contributions to the single-particle energy per nucleon. We have calculated single-particle energies for the ground state of $N = 8$ isotones. Since the monopole interaction between $0p$ orbits is larger than that between the $0p$ orbit and the $1s$ orbit, the large energy gap that corresponds to the magic number $N = 8$ becomes narrower as the proton number decreases from $Z = 8$ to $Z = 2$. Similarly, in the case of $N = 20$ isotones, the large energy gap that corresponds to the magic number $N = 20$ becomes narrower as the proton number decreases from $Z = 20$ to $Z = 8$. In these cases, the neutron-proton monopole interactions play the important role for the change of the neutron single-particle spectrum, when protons are removed from a nucleus.

We have analyzed the monopole interactions from the empirical matrix elements of NN interactions, by making use of tensorial structure of the forces. The analysis of the empirical matrix elements of NN interactions has shown that the triplet-even component of the neutron-proton interactions dominates monopole interactions and consequently determines the change of neutron single-particle energy spectra with proton number. An analysis for a two-nucleon system has suggested that the triplet-even central component is strongly attractive partly because of the original central interaction and partly because of second-order tensor correlations of the OPE potential.

We have performed an alternative analysis of the monopole interaction by a multipole expansion of NN interactions. The strengths of monopole interactions depend on overlaps between form factors of single-particle states under an assumption of the short-range limit of NN interactions. The overlaps between the orbits with the same nodal quantum number are considerably larger than those between the orbits with different nodal quantum numbers. We expect that the contribution to the single-particle energy from the monopole interactions is large between the orbits with the same nodal quantum number, whereas it is small between those with different nodal quantum numbers.

In the empirical interactions, the monopole interaction of the TE channel is larger than that of the SE channel and the monopole interaction of the SO channel is much smaller. These features of the monopole interaction are not explained by the spin-isospin $(\boldsymbol{\sigma} \cdot \boldsymbol{\sigma})(\boldsymbol{\tau} \cdot \boldsymbol{\tau})$ component.

In the near future, experiments for neutron-rich nuclei with $A > 50$ will be carried out in the next-generation radioactive beam facilities such as RIBF at RIKEN [72]. We expect that the analysis methods performed in this paper will be required in these medium-heavy neutron-rich nuclei.

APPENDIX A: DECOMPOSITION METHOD

Here, we describe the decomposition method of the matrix elements given in the jj-coupling isospin formalism, $\langle jj'|\hat{V}|\bar{j}\bar{j}'\rangle_{TJ}$. By making use of tensorial structure of the forces, we can decompose the matrix elements into components of the central, spin-orbit, and tensor forces.

First, we suppose that single-particle states of spin-orbit partners, $j = \ell \pm 1/2$, have the same radial wave function. Then, we can rewrite the jj-coupling matrix elements to the LS coupling, $\langle \Lambda S|\hat{V}|\bar{\Lambda}\bar{S}\rangle_{TJ}$, as

$$\begin{aligned}\langle \Lambda S|\hat{V}|\bar{\Lambda}\bar{S}\rangle_{TJ} = &\sum_{jj'} \sqrt{\frac{1+\delta_{jj'}}{1+\delta_{\ell\ell'}}} [\Lambda][S][j][j'] \begin{Bmatrix} \ell & \ell' & \Lambda \\ \frac{1}{2} & \frac{1}{2} & S \\ j & j' & J \end{Bmatrix} \\ &\times \sum_{\bar{j}\bar{j}'} \sqrt{\frac{1+\delta_{\bar{j}\bar{j}'}}{1+\delta_{\bar{\ell}\bar{\ell}'}}} [\bar{\Lambda}][\bar{S}][\bar{j}][\bar{j}'] \begin{Bmatrix} \bar{\ell} & \bar{\ell}' & \bar{\Lambda} \\ \frac{1}{2} & \frac{1}{2} & \bar{S} \\ \bar{j} & \bar{j}' & J \end{Bmatrix} \\ &\times \langle jj'|\hat{V}|\bar{j}\bar{j}'\rangle_{TJ}, \end{aligned} \quad (A1)$$

where Λ and $\bar{\Lambda}$ are the orbital angular momenta of two-particle systems.

Second, we make use of different tensorial ranks k of central, spin-orbit, and tensor forces. The central force is a sum of products of $k = 0$ spin operator and $k = 0$ orbital

operator. The spin-orbit (tensor) force is a sum of products of $k = 1 (k = 2)$ operators. Because of the difference of these tensorial ranks, we can pick up components of a specific rank k, using the Racah algebra, as

$$\langle \Lambda S|\hat{V}_k|\bar{\Lambda}\bar{S}\rangle_{TJ} = \sum_J (-1)^{J'-J}[J']^2[k]^2 W(\Lambda S\bar{\Lambda}\bar{S}; J'k) \times W(\Lambda S\bar{\Lambda}\bar{S}; Jk)\langle \Lambda S|\hat{V}|\bar{\Lambda}\bar{S}\rangle_{TJ'}, \quad \text{(A2)}$$

where $\hat{V}_{k=0} = \hat{V}_C$, $\hat{V}_{k=1} = \hat{V}_{\rm LS}$, and $\hat{V}_{k=2} = \hat{V}_{\rm TN}$, respectively.

Third, we use quantum numbers of the interaction channels. For example, the SO component of the central force survives only between $S = \bar{S} = 0$ for $T = 0$ channels and vanishes in the other channels. In the same way, the TE, SE, and TO components contribute only in $(S, T) = (1, 0)$, $(0, 1)$, and $(1, 1)$, respectively. Since the spin-orbit and tensor forces have the operators $\hat{\boldsymbol{S}}$ and $\hat{S}_{12}$, respectively, the matrix elements of LSE and TNE components contribute in $(S, T) = (1, 0)$, and those of LSO and TNO components contribute in $(S, T) = (1, 1)$.

Finally, by using the inverse transformation from LS coupling to jj coupling,

$$\langle jj'|\hat{V}|\bar{j}\bar{j}'\rangle_{TJ} = \sum_{\Lambda S}\sqrt{\frac{1+\delta_{\ell\ell'}}{1+\delta_{jj'}}}[\Lambda][S][j][j'] \begin{Bmatrix} \ell & \ell' & \Lambda \\ \frac{1}{2} & \frac{1}{2} & S \\ j & j' & J \end{Bmatrix} \times \sum_{\bar{\Lambda}\bar{S}}\sqrt{\frac{1+\delta_{\bar{\ell}\bar{\ell}'}}{1+\delta_{\bar{j}\bar{j}'}}}[\bar{\Lambda}][\bar{S}][\bar{j}][\bar{j}'] \begin{Bmatrix} \bar{\ell} & \bar{\ell}' & \bar{\Lambda} \\ \frac{1}{2} & \frac{1}{2} & \bar{S} \\ \bar{j} & \bar{j}' & J \end{Bmatrix} \times \langle \Lambda S|\hat{V}|\bar{\Lambda}\bar{S}\rangle_{TJ}, \quad \text{(A3)}$$

we can decompose the matrix elements $\langle jj'|\hat{V}|\bar{j}\bar{j}'\rangle_{TJ}$ into the eight components of Eqs. (49), (52), and (53) in Sec. VI B. Nonvanishing matrix elements with $S \neq \bar{S}$ are obtained from empirical interactions. To describe these matrix elements, we need an antisymmetric spin-orbit force. However, these matrix elements are small and we neglect them.

APPENDIX B: PROCEDURE OF MULTIPOLE EXPANSION

Here, we describe the procedure of the multipole expansion for a central force of an NN interaction. It is sometimes useful to decompose an NN interaction into a sum of products of two one-body operators, one acting on the first nucleon and the other on the second nucleon. Such a decomposition is achieved by a multipole expansion [69]. Here, it is convenient to use the spin/isospin representation

$$\hat{V} = V_0(r) + V_\sigma(r)(\hat{\boldsymbol{\sigma}}_1 \cdot \hat{\boldsymbol{\sigma}}_2) + V_\tau(r)(\hat{\boldsymbol{\tau}}_1 \cdot \hat{\boldsymbol{\tau}}_2) + V_{\sigma\tau}(r)(\hat{\boldsymbol{\sigma}}_1 \cdot \hat{\boldsymbol{\sigma}}_2)(\hat{\boldsymbol{\tau}}_1 \cdot \hat{\boldsymbol{\tau}}_2), \quad \text{(B1)}$$

with $r = |\boldsymbol{r}_1 - \boldsymbol{r}_2|$. The multipole expansion is achieved by the Fourier and its inverse transformations

$$V(r) = \frac{1}{(2\pi)^3}\int d\boldsymbol{p} e^{-i\boldsymbol{p}\cdot\boldsymbol{r}} \int d\boldsymbol{r} e^{i\boldsymbol{p}\cdot\boldsymbol{r}} V(r), \quad \text{(B2)}$$

by using the multipole expansion

$$e^{i\boldsymbol{p}\cdot\boldsymbol{r}} = 4\pi \sum_{k=0}^{\infty} i^k j_k(pr)(\boldsymbol{Y}^{(k)}(\Omega) \cdot \boldsymbol{Y}^{(k)}(\Omega_p)) \quad \text{(B3)}$$

and the orthonormality of spherical harmonics. Here, Ω is the direction of vector $\boldsymbol{r} = \boldsymbol{r}_1 - \boldsymbol{r}_2$, p and Ω_p denote the magnitude and direction of momentum $\boldsymbol{p}$, $j_k(pr)$ are spherical Bessel functions, and $\boldsymbol{Y}^{(k)}$ are spherical harmonics with rank k. Thus, a potential is expressed as a sum of products of two one-body operators, one acting on the first nucleon and the other on the second nucleon:

$$V(r) = \int_0^\infty p^2 dp\, v(p) \sum_k [k]^2 (\boldsymbol{F}^{(k)}(p; \boldsymbol{r}_1) \cdot \boldsymbol{F}^{(k)}(p; \boldsymbol{r}_2)), \quad \text{(B4)}$$

where

$$v(p) = \frac{2}{\pi}\int_0^\infty r^2 dr V(r) j_0(pr) \quad \text{(B5)}$$

is the Fourier-Bessel transform and we define the operator $\boldsymbol{F}^{(k)}(p; \boldsymbol{r}_i)$ as

$$\boldsymbol{F}^{(k)}(p; \boldsymbol{r}_i) = \sqrt{\frac{4\pi}{2k+1}} j_k(pr_i)\, \boldsymbol{Y}^{(k)}(\Omega_i). \quad \text{(B6)}$$

Since the nucleons are distinguished by the labeling, matrix elements of an NN interaction consist of direct and exchange terms,

$$\langle jj'|\hat{V}|jj'\rangle_{TJ} = \langle jj'|\hat{V}|jj'\rangle_{TJ}^{\rm direct} + \langle jj'|\hat{V}|jj'\rangle_{TJ}^{\rm exch}, \quad \text{(B7)}$$

where

$$\langle jj'|\hat{V}|jj'\rangle_{TJ}^{\rm direct} = \frac{1}{1+\delta_{jj'}}\langle j_{(1)}j'_{(2)}|\hat{V}|j_{(1)}j'_{(2)}\rangle_{TJ}, \quad \text{(B8)}$$

$$\langle jj'|\hat{V}|jj'\rangle_{TJ}^{\rm exch} = \frac{-1}{1+\delta_{jj'}}\langle j_{(1)}j'_{(2)}|\hat{V}|j_{(2)}j'_{(1)}\rangle_{TJ}. \quad \text{(B9)}$$

From Eqs. (39), (B8), and (B9), the direct and exchange terms of the neutron-proton monopole interaction are written as

$$\Delta\varepsilon_{jj'}^{\rm direct} = \sum_{TJ}\frac{[J]^2}{2[j]^2[j']^2}\langle j_{(1)}j'_{(2)}|\hat{V}|j_{(1)}j'_{(2)}\rangle_{TJ}, \quad \text{(B10)}$$

$$\Delta\varepsilon_{jj'}^{\rm exch} = \sum_{TJ}\frac{-[J]^2}{2[j]^2[j']^2}\langle j_{(1)}j'_{(2)}|\hat{V}|j_{(2)}j'_{(1)}\rangle_{TJ}, \quad \text{(B11)}$$

respectively.

First, we consider the direct term. By using the multipole expansion, a matrix element of $V_0(r)$ is given by the sum of the products of the operator with $\boldsymbol{r}_1$ and the operator with $\boldsymbol{r}_2$ as

$$\langle j(1)j'(2)|V_0(r)|j(1)j'(2)\rangle_{TJ} = \int_0^\infty p^2 dp v_0(p) \sum_k [k]^2 (-1)^{J-j-j'} W(jj'jj'; Jk) \times \langle j\|\boldsymbol{F}^{(k)}(p; \boldsymbol{r}_1)\|j\rangle\langle j'\|\boldsymbol{F}^{(k)}(p; \boldsymbol{r}_2)\|j'\rangle, \quad \text{(B12)}$$

where the matrix elements of the right-hand side are integrated out with respect to $\boldsymbol{r}_i$, respectively, and are functions of

momentum p. Multiplying each side of Eq. (B12) by $(2J+1)$, summing up J and T, and using the relation

$$\sum_J (-1)^{J-j-j'}[J]^2 W(jj'jj';Jk) = \delta_{k0}[j][j'], \quad \text{(B13)}$$

we obtain

$$\begin{aligned}\sum_{TJ}[J]^2\langle j(1)j'(2)|V_0(r)|j(1)j'(2)\rangle_{TJ} &= \sum_T [j][j']\int_0^\infty p^2 dp v_0(p)\,\phi_j(p)\,\phi_{j'}(p) \\ &= 2[j][j']\int_0^\infty p^2 dp v_0(p)\,\phi_j(p)\,\phi_{j'}(p), \quad \text{(B14)}\end{aligned}$$

where we define the form factor $\phi_j(p)$ as

$$\phi_j(p) = \frac{1}{[j]}\langle j\|\boldsymbol{F}^{(0)}(p;\boldsymbol{r}_i)\|j\rangle = \langle j|j_0(pr)|j\rangle. \quad \text{(B15)}$$

Similarly, in the case of $V_\tau(r)(\boldsymbol{\tau}_1\cdot\boldsymbol{\tau}_2)$, the isospin operator just gives rise to a factor of $(4T-3)$, and we obtain

$$\begin{aligned}\sum_{TJ}[J]^2\langle j(1)j'(2)|V_\tau(r)(\boldsymbol{\tau}_1\cdot\boldsymbol{\tau}_2)|j(1)j'(2)\rangle_{TJ} &= \sum_T (4T-3)[j]^2[j']^2\int_0^\infty p^2 dp v_\tau(p)\,\phi_j(p)\,\phi_{j'}(p) \\ &= -2[j]^2[j']^2\int_0^\infty p^2 dp v_\tau(p)\,\phi_j(p)\,\phi_{j'}(p). \quad \text{(B16)}\end{aligned}$$

In the case of $V_\sigma(r)(\boldsymbol{\sigma}_1\cdot\boldsymbol{\sigma}_2)$, this term is rewritten by recoupling operators $\boldsymbol{F}^{(k)}$ and $\boldsymbol{\sigma}$ as

$$\begin{aligned}V_\sigma(r)(\boldsymbol{\sigma}_1\cdot\boldsymbol{\sigma}_2) = \int_0^\infty p^2 dp v_\sigma(p)\sum_{kk'}[k]^2(-1)^{k+k'+1} &\times([\boldsymbol{F}^{(k)}(p;\boldsymbol{r}_1)\otimes\boldsymbol{\sigma}_1]^{(k')} \\ &\times[\boldsymbol{F}^{(k)}(p;\boldsymbol{r}_2)\otimes\boldsymbol{\sigma}_2]^{(k')}), \quad \text{(B17)}\end{aligned}$$

and we obtain

$$\begin{aligned}\sum_{TJ}[J]^2\langle j(1)j'(2)|V_\sigma(r)(\boldsymbol{\sigma}_1\cdot\boldsymbol{\sigma}_2)|j(1)j'(2)\rangle_{TJ} &= 6[j][j']\int_0^\infty p^2 dp v_\sigma(p)\langle j\|[\boldsymbol{F}^{(1)}(p;\boldsymbol{r}_1)\otimes\boldsymbol{\sigma}_1]^{(0)}\|j\rangle \\ &\times\langle j'\|[\boldsymbol{F}^{(1)}(p;\boldsymbol{r}_2)\otimes\boldsymbol{\sigma}_2]^{(0)}\|j'\rangle. \quad \text{(B18)}\end{aligned}$$

Here, since the operator $\boldsymbol{F}^{(1)}(p;\boldsymbol{r}) = \sqrt{4\pi/3}\,j_1(pr)\,\boldsymbol{Y}^{(1)}(\Omega)$ changes the parity, the matrix elements of Eq. (B18) vanish,

$$\langle j\|[\boldsymbol{F}^{(1)}(p;\boldsymbol{r}_i)\otimes\boldsymbol{\sigma}_i]^{(0)}\|j\rangle = 0. \quad \text{(B19)}$$

Therefore, the $V_\sigma(r)(\boldsymbol{\sigma}_1\cdot\boldsymbol{\sigma}_2)$ component of $\Delta\varepsilon^{\rm direct}_{jj'}$ vanishes. For the same reason, the $V_{\sigma\tau}(r)(\boldsymbol{\sigma}_1\cdot\boldsymbol{\sigma}_2)(\boldsymbol{\tau}_1\cdot\boldsymbol{\tau}_2)$ component does not contribute to $\Delta\varepsilon^{\rm direct}_{jj'}$. In the direct terms, spin-dependent central components do not contribute to the single-particle energies. This restriction is due to parity conservation and angular-momentum coupling of one-body operators and single-particle wave functions. As a result, we obtain the direct term of the neutron-proton monopole interaction,

$$\Delta\varepsilon^{\rm direct}_{jj'} = \int_0^\infty p^2 dp(v_0(p) - v_\tau(p))\phi_j(p)\,\phi_{j'}(p), \quad \text{(B20)}$$

for the central components.

Next, we consider the exchange term. A matrix element of the exchange term is written as

$$\begin{aligned}&\langle j(1)j'(2)|\hat{V}|j(2)j'(1)\rangle_{TJ} \\ &\quad = \langle j(1)j'(2)|\hat{V}\,\hat{P}^r\hat{P}^\sigma\hat{P}^\tau|j(1)j'(2)\rangle_{TJ}, \quad \text{(B21)}\end{aligned}$$

where $\hat{P}^r$, $\hat{P}^\sigma$, and $\hat{P}^\tau$ are exchange operators. The operator $\hat{P}^r$ exchanges the spatial coordinates $\boldsymbol{r}_1$ and $\boldsymbol{r}_2$ of the particles. The operators $\hat{P}^\sigma$ and $\hat{P}^\tau$ are written as

$$\hat{P}^\sigma = \frac{1+\hat{\boldsymbol{\sigma}}_1\cdot\hat{\boldsymbol{\sigma}}_2}{2}, \quad \hat{P}^\tau = \frac{1+\hat{\boldsymbol{\tau}}_1\cdot\hat{\boldsymbol{\tau}}_2}{2} \quad \text{(B22)}$$

and exchange the spin and isospin coordinates, respectively. Since the central force is written as

$$\begin{aligned}\hat{V} &= V_0(r) + V_\sigma(r)(2\hat{P}^\sigma - 1) \\ &\quad + V_\tau(r)(2\hat{P}^\tau - 1) + V_{\sigma\tau}(r)(2\hat{P}^\sigma - 1)(2\hat{P}^\tau - 1) \quad \text{(B23)}\end{aligned}$$

by using the spin and isospin exchange operators, $\hat{V}\,\hat{P}^r\hat{P}^\sigma\hat{P}^\tau$ is written as

$$\begin{aligned}\hat{V}\,\hat{P}^r\hat{P}^\sigma\hat{P}^\tau &= V_0(r)\,\hat{P}^r\hat{P}^\sigma\hat{P}^\tau + V_\sigma(r)\,\hat{P}^r(2-\hat{P}^\sigma)\hat{P}^\tau \\ &\quad + V_\tau(r)\hat{P}^r\,\hat{P}^\sigma(2-\hat{P}^\tau) \\ &\quad + V_{\sigma\tau}(r)\,\hat{P}^r(2-\hat{P}^\sigma)(2-\hat{P}^\tau) \\ &= \left(\frac{V_0(r)+3V_\sigma(r)+3V_\tau(r)+9V_{\sigma\tau}(r)}{4}\right)\hat{P}^r \\ &\quad + \left(\frac{V_0(r)-V_\sigma(r)+3V_\tau(r)-3V_{\sigma\tau}(r)}{4}\right)\hat{P}^r \\ &\quad \times(\hat{\boldsymbol{\sigma}}_1\cdot\hat{\boldsymbol{\sigma}}_2) \\ &\quad + \left(\frac{V_0(r)+3V_\sigma(r)-V_\tau(r)-3V_{\sigma\tau}(r)}{4}\right) \\ &\quad \times\hat{P}^r(\hat{\boldsymbol{\tau}}_1\cdot\hat{\boldsymbol{\tau}}_2) \\ &\quad + \left(\frac{V_0(r)-V_\sigma(r)-V_\tau(r)+V_{\sigma\tau}(r)}{4}\right) \\ &\quad \times\hat{P}^r(\hat{\boldsymbol{\sigma}}_1\cdot\hat{\boldsymbol{\sigma}}_2)(\hat{\boldsymbol{\tau}}_1\cdot\hat{\boldsymbol{\tau}}_2). \quad \text{(B24)}\end{aligned}$$

Because of the exchange operator $\hat{P}^r$, the multipole expansion for the exchange term gives a complicated form. In the case of $V(r) = V_{\rm const}\delta(r)$, this interaction acts only on the relative S state. Then, $\hat{P}^r$ is replaced by $\hat{1}$, and we can derive a simple form such as Eq. (B20) for the direct term. For the interaction $\hat{V}\,\hat{P}^r\hat{P}^\sigma\hat{P}^\tau$, we carry out the multipole expansion in the same way as the direct term, and we obtain

$$\Delta\varepsilon^{\rm exch}_{jj'} = (-v_\tau - 3v_{\sigma\tau})\int_0^\infty p^2 dp\,\phi_j(p)\,\phi_{j'}(p), \quad \text{(B25)}$$

where v_τ and $v_{\sigma\tau}$ are constants that are obtained by the Fourier-Bessel transformation of the δ functions. Therefore, in the exchange term, only the isospin-dependent central components contribute to the neutron-proton monopole interaction. Generally, for $\hat{V}_0(r)$ and $\hat{V}_\sigma(r)(\hat{\boldsymbol{\sigma}}_1\cdot\hat{\boldsymbol{\sigma}}_2)$ components, the sum of the matrix elements,

$$\begin{aligned}&\sum_T\langle j(1)j'(2)|\hat{V}|j(2)j'(1)\rangle_{TJ} \\ &\quad = \sum_T(-1)^{1-T}(-1)^{j+j'-J}\langle j(1)j'(2)|\hat{V}|j'(1)j(2)\rangle_{TJ}, \quad \text{(B26)}\end{aligned}$$

vanishes because of the phase factor $(-1)^{1-T}$. Therefor, $V_0(r)$ and $V_\sigma(r)(\hat{\boldsymbol{\sigma}}_1 \cdot \hat{\boldsymbol{\sigma}}_2)$ do not contribute to the exchange term of the neutron-proton monopole interaction.

[1] F. C. Barker, J. Phys. G **2**, L45 (1976).
[2] F. C. Barker and G. T. Hickey, J. Phys. G **3**, L23 (1977).
[3] D. E. Alburger, S. Mordechai, H. T. Fortune, and R. Middleton, Phys. Rev. C **18**, 2727 (1978).
[4] H. Keller, R. Anne, D. Bazin, R. Bimbot, M. J. G. Borge, J. M. Corre, S. Dogny, H. Emling, D. Guillemaud-Mueller, P. G. Hansen, P. Hornshøj, F. Humbert, P. Jensen, B. Jonson, M. Lewitowicz, A. C. Mueller, R. Neugart, T. Nilsson, G. Nyman, F. Pougheon, M. G. Saint-Laurent, G. Schrieder, O. Sorlin, O. Tengblad, and K. Wilhelmsen Rolander, Z. Phys. A **348**, 61 (1994).
[5] H. Simon, D. Aleksandrov, T. Aumann, L. Axelsson, T. Baumann, M. J. G. Borge, L. V. Chulkov, R. Collatz, J. Cub, W. Dostal, B. Eberlein, T. W. Elze, H. Emling, H. Geissel, A. Grünschloss, M. Hellström, J. Holeczek, R. Holzmann, B. Jonson, J. V. Kratz, G. Kraus, R. Kulessa, Y. Leifels, A. Leistenschneider, T. Leth, I. Mukha, G. Münzenberg, F. Nickel, T. Nilsson, G. Nyman, B. Petersen, M. Pfützner, A. Richter, K. Riisager, C. Scheidenberger, G. Schrieder, W. Schwab, M. H. Smedberg, J. Stroth, A. Surowiec, O. Tengblad, and M. V. Zhukov, Phys. Rev. Lett. **83**, 496 (1999).
[6] A. Poves and J. Retamosa, Phys. Lett. **B184**, 311 (1987).
[7] T. Motobayashi, Y. Ikeda, Y. Ando, K. Ieki, M. Inoue, N. Iwasa, T. Kikuchi, M. Kurokawa, S. Moriya, S. Ogawa, H. Murakami, S. Shimoura, Y. Yanagisawa, T. Nakamura, Y. Watanabe, M. Ishihara, T. Teranishi, H. Okuno, and R. F. Casten, Phys. Lett. **B346**, 9 (1995).
[8] A. Ozawa, T. Kobayashi, T. Suzuki, K. Yoshida, and I. Tanihata, Phys. Rev. Lett. **84**, 5493 (2000).
[9] Y. Yanagisawa, M. Notani, H. Sakurai, M. Kunibu, H. Akiyoshi, N. Aoi, H. Baba, K. Demichi, N. Fukuda, H. Hasegawa, Y. Higurashi, M. Ishihara, N. Iwasa, H. Iwasaki, T. Gomi, S. Kanno, M. Kurokawa, Y. U. Matsuyama, S. Michimasa, T. Minemura, T. Mizoi, T. Nakamura, A. Saito, M. Serata, S. Shimoura, T. Sugimoto, E. Takeshita, S. Takeuchi, K. Ue, K. Yamada, K. Yoneda, and T. Motobayashi, Phys. Lett. **B566**, 84 (2003).
[10] M. Stanoiu, F. Azaiez, Z. Dombŕdi, O. Sorlin, B. A. Brown, M. Belleguic, D. Sohler, M. G. Saint Laurent, M. J. Lopez-Jimenez, Y. E. Penionzhkevich, G. Sletten, N. L. Achouri, J. C. Angélique, F. Becker, C. Borcea, C. Bourgeois, A. Bracco, J. M. Daugas, Z. Dlouhý, C. Donzaud, J. Duprat, Z. Fülöp, D. Guillemaud-Mueller, S. Grévy, F. Ibrahim, A. Kerek, A. Krasznahorkay, M. Lewitowicz, S. Leenhardt, S. Lukyanov, P. Mayet, S. Mandal, H. van der Marel, W. Mittig, J. Mŕzek, F. Negoita, F. De Oliveira-Santos, Z. Podolyk, F. Pougheon, M. G. Porquet, P. Roussel-Chomaz, H. Savajols, Y. Sobolev, C. Stodel, J. Timŕ, and A. Yamamoto, Phys. Rev. C **69**, 034312 (2004).
[11] I. Talmi and I. Unna, Phys. Rev. Lett. **4**, 469 (1960).
[12] K. Heyde and J. L. Wood, J. Phys. G **17**, 135 (1991).
[13] Y. Utsuno, T. Otsuka, T. Mizusaki, and M. Honma, Phys. Rev. C **60**, 054315 (1999).
[14] T. Otsuka, R. Fujimoto, Y. Utsuno, B. A. Brown, M. Honma, and T. Mizusaki, Phys. Rev. Lett. **87**, 082502 (2001).
[15] I. Hamamoto, S. V. Lukyanov, and X. Z. Zhang, Nucl. Phys. **A683**, 255 (2001).
[16] H. Grawe, Acta Phys. Pol. B **34**, 2267 (2003).
[17] A. Umeya and K. Muto, Balkan Phys. Lett., special issue, 329 (2006).
[18] A. Umeya and K. Muto, Phys. Rev. C **69**, 024306 (2004).
[19] A. Umeya and K. Muto, in *Proceedings of International Symposium on "Spin and Quantum Structure in Hadrons, Nuclei, and Atoms (SQS04),"* edited by K. Asahi and T. Shibata (Tokyo Institute of Technology, Tokyo, 2004), p. 74.
[20] G. Audi and A. H. Wapstra, Nucl. Phys. **A595**, 409 (1995).
[21] S. Raman, C. H. Malarkey, W. T. Milner, C. W. Nestor Jr., and P. H. Stelson, At. Data Nucl. Data Tables **36**, 1 (1987).
[22] P. M. Endt, Nucl. Phys. **A521**, 1 (1990).
[23] R. W. Ibbotson, T. Glasmacher, B. A. Brown, L. Chen, M. J. Chromik, P. D. Cottle, M. Fauerbach, K. W. Kemper, D. J. Morrissey, H. Scheit, and M. Thoennessen, Phys. Rev. Lett. **80**, 2081 (1998).
[24] S. Raman, C. W. Nestor Jr., and K. H. Bhatt, Phys. Rev. C **37**, 805 (1988).
[25] S. Raman, C. W. Nestor Jr., and P. Tikkanen, At. Data Nucl. Data Tables **78**, 1 (2001).
[26] J. B. French, in *Proceedings of International School of Physics Enrico Fermi, Cource 36, Varenna 1965,* C. Bloch, directer (Academic Press, New York, 1966).
[27] M. Baranger, Nucl. Phys. **A149**, 225 (1970).
[28] M. H. Macfarlane and J. B. French, Rev. Mod. Phys. **32**, 567 (1960).
[29] A. Terakawa, T. Tohei, T. Nakagawa, A. Sato, J. Takamatsu, M. Mori, A. Narita, H. Orihara, K. Ishii, T. Niizeki, M. Oura, S. Hirasaki, M. Hosaka, G. C. Jon, K. Miura, and H. Ohnuma, Phys. Rev. C **48**, 2775 (1993).
[30] G. Mairle, L. K. Pao, G. J. Wagner, K. T. Knöpfle, and H. Riedsel, Z. Phys. A **301**, 157 (1981).
[31] G. Th. Kaschl, G. J. Wagner, G. Mairle, U. Schmidt-Rohr, and P. Turek, Nucl. Phys. **A155**, 417 (1970).
[32] G. Mairle, G. J. Wagner, K. T. Knöpfle, L. K. Pao, H. Riedsel, V. Bechtold, and L. Friedrich, Nucl. Phys. **A363**, 413 (1981).
[33] R. K. Bansal and J. B. French, Phys. Lett. **11**, 145 (1964).
[34] A. Poves and A. Zuker, Phys. Rep. **70**, 235 (1981).
[35] S. Cohen and D. Kurath, Nucl. Phys. **73**, 1 (1965).
[36] B. H. Wildenthal, Prog. Part. Nucl. Phys. **11**, 5 (1984).
[37] D. J. Millener and D. Kurath, Nucl. Phys. **A255**, 315 (1975).
[38] J. Blomqvist and A. Molinari, Nucl. Phys. **A106**, 545 (1968).
[39] J. B. McGrory, Phys. Rev. C **8**, 693 (1973).
[40] J. P. Schiffer and W. W. True, Rev. Mod. Phys. **48**, 191 (1976).
[41] H. Grawe, A. Blazhev, M. Górska, I. Mukha, C. Plettner, E. Roeckl, F. Nowacki, R. Grzywacz, and M. Sawicka, Eur. Phys. J. A **25**, s01 357 (2005).
[42] H. Grawe, A. Blazhev, M. Górska, R. Grzywacz, H. Mach, and I. Mukha, Eur. Phys. J. A **27**, s01 257 (2006).
[43] H. Grawe, Springer Lecture Notes Phys. **651**, 33 (2004).
[44] G. Audi, O. Bersillon, J. Blachot, and A. H. Wapstra, Nucl. Phys. **A729**, 3 (2003).
[45] J. Blomqvist and L. Rydström, Phys. Scr. **31**, 31 (1985).
[46] T. T. S. Kuo and G. E. Brown, Nucl. Phys. **A114**, 241 (1968).

[47] T. T. S. Kuo and G. E. Brown, Nucl. Phys. **85**, 40 (1966).
[48] R. V. Reid, Ann. Phys. (NY) **50**, 411 (1968).
[49] M. Lacombe, B. Loiseau, J. M. Richard, R. Vinh Mau, J. Côté, P. Pirès, and R. de Tourreil, Phys. Rev. C **21**, 861 (1980).
[50] R. Machleidt, Advances in Nuclear Physics, Vol. 19, edited by J. W. Negele and E. Vogt (Academic, New York, 1989), Chap. 2.
[51] J. R. Bergervoet, P. C. van Campen, R. A. M. Klomp, J.-L. de Kok, T. A. Rijken, V. G. J. Stoks, and J. J. de Swart, Phys. Rev. C **41**, 1435 (1990).
[52] A. P. Zuker, B. Buck, and J. B. McGrory, Phys. Rev. Lett. **21**, 39 (1968).
[53] A.P. Zuker, Phys. Rev. Lett. **23**, 983 (1969).
[54] E. Caurier, G. Martínez-Pinedo, F. Nowacki, A. Poves, and A. P. Zuker, Rev. Mod. Phys. **77**, 427 (2005).
[55] K. Suzuki and R. Okamoto, Prog. Theor. Phys. **92**, 1045 (1994).
[56] J. Iwadare, S. Otsuki, R. Tamagaki, and W. Watari, Supplement of the Progress of Theoretical Physics **3**, 32 (1956).
[57] R. Tamagaki and W. Watari, Supplement of the Progress of Theoretical Physics **39**, 23 (1967).
[58] K. Shimizu, M. Ichimura, and A. Arima, Nucl. Phys. **A226**, 282 (1974).
[59] I. S. Towner and F. C. Khanna, Phys. Rev. Lett. **42**, 51 (1979).
[60] I. S. Towner and F. C. Khanna, Nucl. Phys. **399**, 334 (1983).
[61] K. Suzuki and R. Okamoto, Prog. Theor. Phys. **75**, 1388 (1986).
[62] K. Suzuki and R. Okamoto, Prog. Theor. Phys. **76**, 127 (1986).
[63] K. Suzuki, R. Okamoto, and H. Kumagai, Prog. Theor. Phys. **77**, 196 (1987).
[64] A. P. Zuker, Phys. Rev. Lett. **91**, 179201 (2003).
[65] A. P. Zuker, Nucl. Phys. **A576**, 65 (1994).
[66] J. Duflo and A. P. Zuker, Phys. Rev. C **59**, R2347 (1999).
[67] T. Otsuka, T. Suzuki, R. Fujimoto, H. Grawe, and Y. Akaishi, Phys. Rev. Lett. **95**, 232502 (2005).
[68] T. Otsuka, T. Suzuki, R. Fujimoto, D. Abe, H. Grawe, and Y. Akaishi, Acta Phys. Pol. B **36**, 1213 (2005).
[69] H. Horie and K. Sasaki, Prog. Theor. Phys. **25**, 475 (1961).
[70] M. S. Antony, J. Britz, J. B. Bueb, and A. Pape, At. Data Nucl. Data Tables **33**, 447 (1985).
[71] S. Nakamura, K. Muto, T. Oda, Nucl. Phys. **A575**, 1 (1994).
[72] T. Motobayashi, Nucl. Instrum. Methods B **204**, 736 (2003).